Technical Note: Lessons from and best practices for the deployment of the Soil Water Isotope Storage System

Rachel E. Havranek [1], Kathryn Snell[1], Sebastian Kopf[1], Brett Davidheiser-Kroll[2], Valerie Morris[3], Bruce Vaughn[3]

Rachel Havranek, Kathryn Snell, Sebastian Kopf, Brett Davidheiser-Kroll, Valerie Morris, Bruce Vaughn

[1]Geological Sciences, University of Colorado Boulder, Boulder, 80303, USA

[2]Thermo Fisher Scientific (Bremen) GmbH, Bremen, Germany

[3]Institute of Arctic and Alpine Research, University of Colorado Boulder, Boulder, 80303, USA

Correspondence to: Rachel Havranek (rachel.havranek@colorado.edu)

Abstract. Soil water isotope datasets are useful for understanding connections between the hydrosphere, atmosphere, biosphere, and geosphere. However, they have been underproduced because of technical challenges associated with collecting those datasets. Here, we present the ~~full~~ results of testing and automation of the Soil Water Isotope Storage System (SWISS). The unique innovation of the SWISS is that we are able to automatically collect water vapor from the critical zone at a regular time interval and then store that water vapor until it can be measured back in a laboratory setting. Through a series of quality assurance and quality control tests, we ~~rigorously~~ tested that the SWISS is resistant to both atmospheric intrusion and leaking in both laboratory and field settings. We assessed the accuracy and precision of the SWISS through a series of experiments where water vapor of known composition was introduced into the flasks, stored for 14 days, and then measured. From these experiments, after applying an offset correction to report our values relative to VSMOW, we assess the precision of the SWISS at ± 0.9‰ and ± 3.7‰ for $\delta^{18}O$ and δ^2H, respectively. We deployed three SWISS units to three different field sites to demonstrate that the SWISS stores water vapor reliably enough that we are able to differentiate dynamics both between the sites as well within a single soil column. Overall, we demonstrate that the SWISS ~~is able to~~can ~~reliably faithfully~~ retains the stable isotope composition of soil water vapor for long enough to allow researchers to address a wide range of ecohydrologic questions.

1 Introduction

Understanding soil water dynamics across a range of environments and soil properties is critical to food and water security (e.g. Mahindawansha et al., 2018; Quade et al., 2019; Rothfuss et al., 2021); understanding biogeochemical cycles, such as the nitrogen and phosphorus cycles (e.g. Hinckley et al., 2014; Harms and Ludwig, 2016); and understanding connections between the hydrosphere, biosphere, geosphere and atmosphere (e.g. Vereeken et al., 2022). One approach that can be used to understand water use and movement in the critical zone is the stable isotope geochemistry of soil water (e.g. Sprenger et al., 2016; Bowen et al., 2019). Variations in the stable isotope ratios of oxygen and hydrogen of soil water ($\delta^{18}O$, δ^2H) track physical processes like infiltration, root water uptake and evaporation. In particular, stable water isotopes are useful for disentangling complex mixtures of water from multiple sources (e.g. Dawson and Ehleringer, 1991; Brooks et al., 2010; Soderberg et al., 2012; Good et al., 2015; Bowen et al., 2018; Gomez-Navarro et al., 2019; Sprenger and Allen 2020). Despite the long-recognized utility of measuring soil water isotopes for understanding a range of processes (e.g. Zimmerman

42   et al., 1966; Peterson & Fry., 1987), soil water isotope datasets have been under-produced as
43   compared to groundwater and meteoric water isotope datasets (Bowen et al., 2019).
44   The primary barrier to producing soil water isotope datasets has been the arduous nature
45   of collecting samples. Historically, there are two primary methods for collecting soil water
46   samples: either by digging a pit and collecting a mass of soil to bring back to the lab for
47   subsequent water extraction or via lysimeter. The former method disrupts the soil profile each
48   time a sample is collected, inhibiting the creation of long-term records of soil water isotopes.
49   Lysimeters on the other hand provide the means to collect multi-year soil water isotope datasets
50   (e.g. Green et al., 2015; Groh et al., 2018; Hinkley et al., 2014; Stumpp et al., 2012, Zhao et al.,
51   2013), but the choice of lysimeter can affect the portion of soil water (i.e. mobile vs. bound) that
52   is sampled (Hinkley et al., 2014; Sprenger et al., 2015) and the soil conditions that are
53   sampleable (i.e. saturation state). Soil water samples collected from both from bulk soil samples
54   and from lysimeters often require manual intervention at the time of sampling.
55   Building off of innovations in laser-based spectroscopy for stable isotope geochemistry,
56   the ecohydrology community developed a variety of in situ soil water sampling methods over the
57   last 15 years that enables the creation of high throughput, high precision analyses of soil water
58   isotopes (e.g. Wassenaar et al., 2008; Gupta et al. 2009; Rothfuss et al., 2013; Volkmann and
59   Weiler, 2014; Gaj et al., 2015; Oerter et al., 2016; Beyer et al., 2020; Kübert et al., 2020). These
60   methods have shed light on provided insights into a range of ecohydrologic questions from
61   evaporation and water use dynamics in managed soils (e.g. Oerter et al., 2017; Quade et al.,
62   2018) to better understanding where plants and trees source their water (e.g. Beyer et al., 2020).
63   These innovations have allowed researchers to ask new questions about ecohydrologic dynamics,
64   but current methods require field deployments of laser-based instruments. Field deployments are
65   technically possible and have been conducted successfully (e.g. Gaj et al., 2016; Volkmann et al.,
66   2016; Oerter et al., 2017; Quade et al., 2019; Künhammer et al.,2021; Seeger and Weiler., 2021;
67   Gessler et al., 2022), but require uninterrupted AC power, adequate shelter, as well as safe and
68   stable operating environments for best results. These prerequisites are not often auna available at
69   mostmany field sites, especially in more remote locations and for longer sampling time frames.
70   Given these logistical constraints, these studies have mostly been done near the institutions
71   performing those studies. Traditionally, soil water samples are taken by digging a pit, and
72   collecting a mass of soil to bring back to the lab for subsequent water extraction, disrupting the
73   soil profile each time a sample is collected. To circumvent issues related to this style of
74   sampling, the ecohydrology community has developed a variety of in situ water sampling
75   methods over the last 10 years (e.g. Rothfuss et al., 2013; Volkmann and Weiler, 2014; Gaj et al.,
76   2015; Oerter et al., 2016; Beyer et al., 2020). These methods have helped to shed light on a range
77   of ecohydrologic questions from evaporation and water use dynamics in managed soils (e.g.
78   Oerter et al., 2017; Quade et al., 2019) to better understanding where plants and trees source their
79   water (e.g. Beyer et al., 2020).
80   The expansion in situ sampling methods allows for a greater understanding of
81   ecohydrologic dynamics temporally, but with current methods these studies are often done in
82   close proximity to the institutions performing the studies because of logistical constraints. The
83   Sspatial constraints limit the questions that researchers can ask about what we can learn about
84   soil hydrology in remote and traditionally understudied landscapes. For example, in the
85   geoscience community there is significant interest in improving the research community's
86   understanding of how and when paleoclimate proxies (e.g. stable isotope records from pedogenic
87   carbonate, branched glycerol dialkyl glycerol tetraethers, etc.) form in soils, because that informs

88 our ability to accurately interpret records from the geologic past. ~~But~~However, those projects
89 commonly have environmental constraints like soil type or local climate ~~state~~characteristics that
90 may not be located near institutions performing those studies. To be able to study a broader
91 range of questions about ecohydrology, there is a need for a system that is capable of
92 autonomously collecting soil water vapor for isotopic analysis in remote settings.
93 ~~Beyond the ecohydrology community, the creation of high temporal resolution soil water~~
94 ~~isotope data sets is useful to a broader set of stakeholders. For example, long-term temporal~~
95 ~~records of soil water can be used to better understand geologic proxy development (e.g. stable~~
96 ~~isotope records from pedogenic carbonate, br-GDGTs, etc.). These projects, however, commonly~~
97 ~~have environmental constraints like soil type or local climate state that may not be located near~~
98 ~~institutions performing those studies, creating the need for a system that is capable of collecting~~
99 ~~water vapor from remote settings in an automated way.~~
100 In this contribution, we report on the further development and testing of a field
101 deployable system called ~~first introduced in Havranek et al., (2020)~~the Soil Water Isotope
102 Storage System (SWISS). The SWISS was built to be paired with ACCURELL PP V8/2HF
103 vapor permeable probes that have been previously tested for soil water isotope applications
104 (Rothfuss et al., 2013; Oerter et al., 2017). Our system uses three basic components to store
105 water vapor produced by the vapor permeable probes: glass flasks, stainless steel tubing and a
106 flask selector valve (Fig. 1, Supplemental Table 1). ~~.~~Previously, we demonstrated through a
107 series of lab experiments that the glass flasks used in the SWISS unit~~s~~s can reliably store water
108 vapor for up to 30 days (Havranek et al., 2020). That proof-of-concept study demonstrated that
109 the flasks retain original water isotope values, but the laboratory system was not field deployable
110 ~~or~~ and did not have customizable automation. Here, we present a fully autonomous, field-ready
111 system that has been ~~thoroughly~~ tested under both laboratory conditions and field conditions,
112 including development and testing of a solar-powered, battery backed automation system that
113 enables pre-scheduled water vapor sampling without manual intervention in remote field
114 locations.
115
116 To test the accuracy and precision of the SWISS, we completed quality assurance and
117 quality control (QA/QC) tests. ~~This system is now capable of independently sampling soil water~~
118 ~~vapor in situ, storing that water vapor for a period of time until the samples can be brought back~~
119 ~~to a laboratory to be measured. In our case, we used a Picarro L-2130i water isotope analyzer~~
120 ~~(Picarro, Inc. Santa Clara, CA) to measure both water concentration and the oxygen and~~
121 ~~hydrogen isotope ratios of the soil water vapor. i water isotope analyzer (Picarro, Inc. Santa~~
122 ~~Clara, CA) to measure both water concentration and the oxygen and hydrogen isotope ratios of~~
123 ~~the soil water vapor. Here, we present the testing and optimization of the Soil Water Isotope~~
124 ~~Storage System (SWISS). First, we present a quality assurance and quality control (QA/QC)~~
125 ~~procedure that we strongly recommend any future user to complete prior to deploying this kind~~
126 ~~of system for either a field or lab experiment. Second~~Here, we demonstrate the viability of this
127 system under field-conditions through two field suitability experiments. ~~Lastly~~In addition, we
128 sampled three different field sites to show that the automation schema works on a monthly
129 timescale and that the system preserves soil water vapor isotope~~s~~ signals with sufficient precision
130 to distinguish between three different field settings and vertical profile differences.

2 ~~Background~~Field Sites

~~In recent years, a number of technical innovations have made it easier to sample and measure soil water for stable isotope analysis. Advances in laser-based instrumentation (e.g. cavity ring-down spectroscopy, CRDS) have made high throughput, high precision measurements of both water concentration and water stable isotopes possible. Field deployments with laser-based instruments are technically possible and have been conducted successfully (e.g. Oerter et al., 2017; Quade et al., 2019; Künhammer et al.,2021), but require uninterrupted AC power, adequate shelter as well as safe and stable operating environments for best results. These prerequisites are not often available at most field sites, especially in more remote locations and for longer sampling time frames.~~
~~Second, the testing and adoption of vapor permeable tubing provides a way to sample soil water vapor with minimal disturbance to the soil profile (e.g. Rothfuss et al., 2013; Quade et al., 2018; Oerter and Bowen, 2019; Beyer et al., 2020; Kubert et al., 2020). This method works by flushing dry nitrogen (or dry air) through the vapor permeable membrane (Accurrell PP V8/2HF, 3M, Germany), creating a water vapor gradient from inside the probe to the soil, thus inducing water vapor movement across the membrane. Water vapor is then entrained in the dry nitrogen and flushed to either a CRDS system or into a storage container. The adoption of vapor permeable tubing has been a large step forward for the ecohydrology community, and opened the possibility of creating long-term soil water stable isotope records, particularly when paired with measurement in the field by spectroscopic instruments. While this application is a major advancement, it has many practical limitations for remote field sites, therefore, we aimed to develop a system, termed the SWISS, that is capable of independently collecting samples and can then store those samples for a period of time before being returned to the lab for analysis.~~

~~**2.1 Soil Water Isotope Storage System details and previous work**~~
~~The Soil Water Isotope Storage System (SWISS) uses three basic components for water vapor storage of multiple samples: glass flasks, stainless steel tubing and a flask selector valve (Fig. 1, Supplementary Table 1). The ability of the SWISS to reliably store water vapor for up to 30 days was demonstrated previously using a series of lab experiments (Havranek et al., 2020). This proof of concept demonstrated that the flasks retain original water isotope values, but the laboratory system was not field deployable or have customizable automation. Here, we present a fully autonomous, field-ready system that has been thoroughly tested under both laboratory conditions and field conditions, including development and testing of a solar-powered, battery backed automation system that enables pre-scheduled water vapor sampling without manual intervention in remote field locations.~~

~~**2.2 Field Sites:**~~
2.~~1~~2.1 Site Set-Up
~~In figure 1 we show the field-setup employed at all of our field sites.~~ At each site we dug two holes~~;~~ ~~In~~ figure 1 ~~we~~ shows the field-setup employed at all of our field sites. ~~.~~ One hole ~~i~~was instrumented with soil moisture and temperature data loggers at 25 cm, 50 cm, 75 cm, and 100 cm depths, as well as the water vapor permeable probes at 25 cm, 50 cm and 75 cm depths (Fig 1A). We deployed a~~A~~ll probes ~~were deployed~~ >9 months before the first samples were collected to allow the soil to settle and return to natural conditions as much as possible. This timeframe

175 iwas longer than other studies (e.g. Kübert et al., 2020) and includeds infiltration of spring and
176 early summer precipitation. -During probe deployment we took care to retain the original soil
177 horizon sequence and horizon depths as much as possible. In the The second hole, is wherewe
178 stored the SWISS unit, dry nitrogen tank, and associated components to power the SWISS are
179 stored (Fig 1B). The water vapor probes, which connected to the SWISS unitss with Bev-A-Line
180 impermeable tubing, awere run through a PVC pipe buried at approximately 15 cm depth. We
181 chose to raun the impermeable tubing underground to limit the effect of diurnal temperature
182 variability on the impermeable tubing, so as to limitprevent condensation as water travels from
183 the relatively warm soil to the SWISS.
184
185
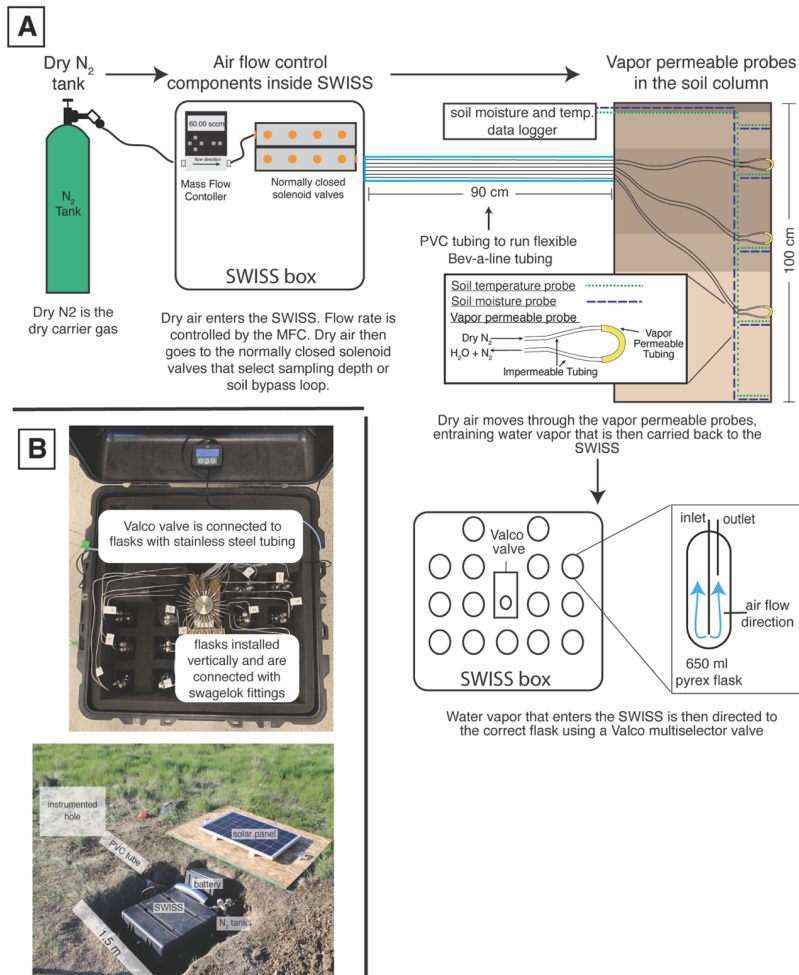
186
Figure 1. A) The sampling flow path. To sample soil water, dry nitrogen is regulated at a specific rate
188 using a mass flow controller, and then directed to one of the three sampling depths, or the soil bypass loop
189 using a set of solenoid valves. Both the mass flow controller and solenoid valves are housed inside the
190 SWISS. Once directed to the correct sampling depth, dry nitrogen is carried to the vapor permeable
191 probes via gas impermeable tubing that is buried approximately 15 cm depth. After passing through the
192 vapor permeable probe, the entrained soil water vapor is carried back to the SWISS where it is directed to
193 the correct flask using a Valco multiselector valve. B) Photos of a built-out SWISS and the layout of a
194 field site. Each of the system components (i.e. solar panel, battery, N_2 tank, SWISS, PVC tube) are
195 labeled, in addition to the location of the instrumented hole in which all of the probes are buried. The hole
196 which houses the SWISS, power, and N_2 tank is approximately 1.5 m wide.

197
198 *much as possible. The second hole is where the SWISS unit, dry nitrogen tank, and associated*
199 *components to power the SWISS are stored (Fig 1B). The water vapor probes, which connect*
200 *to the SWISS with Bev-A-Line impermeable tubing, are run through a PVC pipe buried at*
201 *approximately 15 cm depth. We chose to run the impermeable tubing to the SWISS*
202 *underground to limit the effect of diurnal temperature variability on the impermeable tubing,*
203 *so as to limit condensation as water travels from the relatively warm soil to the SWISS.*
204
2.2.2 Site descriptions

We deployed the SWISS at three field locations: Oglala National Grassland, Nebraska, USA; Briggsdale, Colorado, USA; and Seibert, Colorado, USA.

The Oglala National Grassland site (Lat: 42.9600/Long:, -103.5979/elev: 1117 m) is located in northwestern Nebraska, USA in a cold semi-arid climate. The soil at this site is described as an Aaridisol with a silt-loam texture. It is part of the Olney series (Natural Resources Conservation Service, 2022).

The Briggsdale site (Lat: 40.5947/Long: -104.3190/elev: 1480 m) is located in northeastern Colorado, USA in a cold semi-arid climate. The soil at this site is described as an Aalfisol with a loamy sand - sandy loam texture. It is part of the Olnest series (Natural Resources Conservation Service, 2022). Long term meteorological data from the Briggsdale site is available from the co-located CoAgMet site (CoAgMet, Colorado Climate Center).

The Seibert site (Lat: 39.1187/Long: -102.9250/Elev: 1479 m) is located in eastern Colorado, USA in a cold semi-arid climate. The soil at this site has been described as an Aalfisol, that has a sand loam texture in the top 50 cm of the profile, and a silt loam texture between 50 - 100 cm. It is part of the Stoneham series (Natural Resources Conservation Service, 2022). Long term meteorological data from the site is available from the co-located CoAgMet site (CoAgMet, Colorado Climate Center).

3 Materials

3.1 SWISS Hardware components

In each SWISS there are 15 custom made ~650 ml flasks. These flasks are designed similarly to those used for other water vapor applications. For example, a similar flask is currently used in an unmanned aerial vehicle to collect atmospheric water vapor samples for stable isotope analysis (Rozmiarek et al., 2021). The flasks have one long inlet tube that extends into the flask almost to the base, and one shorter outlet tube so that vapor exiting the flask is well mixed and representative of the whole flask (Fig. 1A). The large flask volume is advantageous because there is a low glass surface area to volume ratio, and therefore we are able to reliably measure vapor from the flasks on a CRDS instrument without interacting with vapor bound to the flask walls. The 15 glass flasks are connected to a 16-port, multi-selector Valco valve. We chose to use a Valco valve because these have previously been shown to sufficiently seal off sample volumes for subsequent stable isotope analysis (Theis et al., 2004). The valve and flasks are connected by ⅛ 1/8 inch stainless steel tubing and stainless steel 1/4 ¼ inch to 1/8 ⅛ inch union Swagelok fittings; we use PTFE ferrules on the glass flasks with the Swagelok fittings. The first port of the Valco valve is 1/8th inch stainless steel tubing that serves as a flask bypass loop, which enables flushing of either dry air or water vapor through the system without interacting with a flask. All components are contained in a 61 cm x 61 cm x 61 cm Pelican case (Pelican 0370) with 3 three layers of Pick n' Pluck foam and convoluted foam (Pelican Products

242 Inc., Torrance, Ca, USA). This case is thermally ~~insulated, and~~insulated and provides enough
243 protection to ~~allow reliable~~safely transport ~~of~~ the SWISS by vehicle to field sites.
244
245 **3.2 Soil Probes**
246   There are three components for the collection and ~~interpretation~~analysis of soil water
247 vapor: vapor permeable probes, soil temperature loggers, and soil moisture sensors (Fig 1B,
248 ~~Supp~~Supplemental~~.~~ Table 1).
249   Here, we use a vapor permeable membrane (~~A~~accu~~r~~rell PP V8/2HF, 3M, Germany) that
250 was first tested for soil water isotope applications by Rothfuss et al., (2013). ~~-~~This method works
251 by flushing dry nitrogen (or dry air) through the vapor permeable membrane, creating a water
252 vapor concentration gradient from inside the probe to the soil, thus inducing water vapor
253 movement across the membrane. Water vapor is then entrained in the dry nitrogen and flushed to
254 either a CRDS system or into a storage container. We opted to use this tubing because it has been
255 shown to deliver reliable data over time (i.e. Rothfuss et al., 2015; Oerter et al., 2019; Kübert et
256 al., 2020; Seeger and Weiler, 2021; Gessler et al,. 2021), and it is easy to use and customize to
257 individual needs (Beyer et al., 2020; Kübert et al., 2020). We previously observed that variability
258 in the length of the vapor permeable tubing can lead to systematic offsets in the stable isotope
259 composition of measured waters that arise from ~~ity~~variability of~~e~~ vapor permeable tube surface
260 area (Havranek et al., 2020). Therefore, we were careful to construct all probes such that the
261 length of the Accurrell vapor permeable tubing was 10 cm long, and the impermeable Bev-A-
262 Line IV connected on each side of the vapor permeable tubing was 2 m long. We cut the Bev-A-
263 Line connections to identical lengths to control for memory effect and to treat all samples
264 identically. We also constructed the vapor permeable probes to be used in the lab setting for
265 standards in an identical fashion.
266   Soil temperature loggers (Onset HOBO MX2201), used for applying a temperature
267 correction to all soil water vapor data and to provide key physical parameters of the soils for
268 other goals beyond this study, were buried at the same depths as the vapor permeable probes.
269 Soil moisture sensors (Onset S-SMD-M005) were also buried at the same depths as the vapor
270 permeable probes.
271
272 **3. 3 Automation components, code style, and remote setting power**
273   The philosophy behind the automation of the SWISS was to make it as easy to reproduce
274 as possible, and as flexible as possible to meet different users' sampling needs. We therefore use
275 widely available hardware components and electronics parts; for each product there are
276 numerous alternatives which should be equally viable and could be swapped to better meet each
277 user's needs. In an effort to make our system as accessible and customizable as possible for the
278 scientific community, all automation code is completely open source and will continue to be
279 refined for future applications and hardware improvements. We note that all code is provided as~~-~~
280 is and should be tested carefully for use in other experiments.
281   The overall sampling scheme used in this paper is described in figure 2 and table 1. Our
282 experimental goal was to create a time series of soil water vapor data from three discrete
283 sampling depths (25 cm, 50 cm, 75 cm). Prior to sampling any soil water vapor, we bypassed the
284 soil probes and flushed the lines within the SWISS. ~~flushed away any water vapor present in the~~
285 ~~lines within the SWISS prior to flushing the sample loops.~~ Then, at the start of sampling for each
286 depth, we also flushed the water vapor probe ~~-~~to remove condensation or 'old' water vapor. The

287 gas from both of those steps was expelled via the flask bypass loop. Each soil depth was then
288 sampled for 45 minutes by flushing through the next flask designated in the sequence.
289   Supplemental fFigure SI 1 shows the components of the automation system. To automate
290 and program the sampling scheme, we used: (1) a microcontroller to run the automation script;
291 (2) a coin-cell battery powered real time clock so that the microcontroller was always capable of
292 keeping track of time through power losses, and therefore maintain the sampling schedule; (3) an
293 RS-232 to TTL converter for serial communication with the Valco valve; (4) solenoid valves that
294 were used to control which depth was being sampled and the associated direct current (VDC)
295 power relay; (5) a mass flow controller used to control the rate at which dry nitrogen (1 ppm
296 H_2O) is flushed through the probes; and (6) a power relay used to power the Valco valve and
297 mass flow controller. All parts are described in detail in Supplemental Table 2.
298
299

300
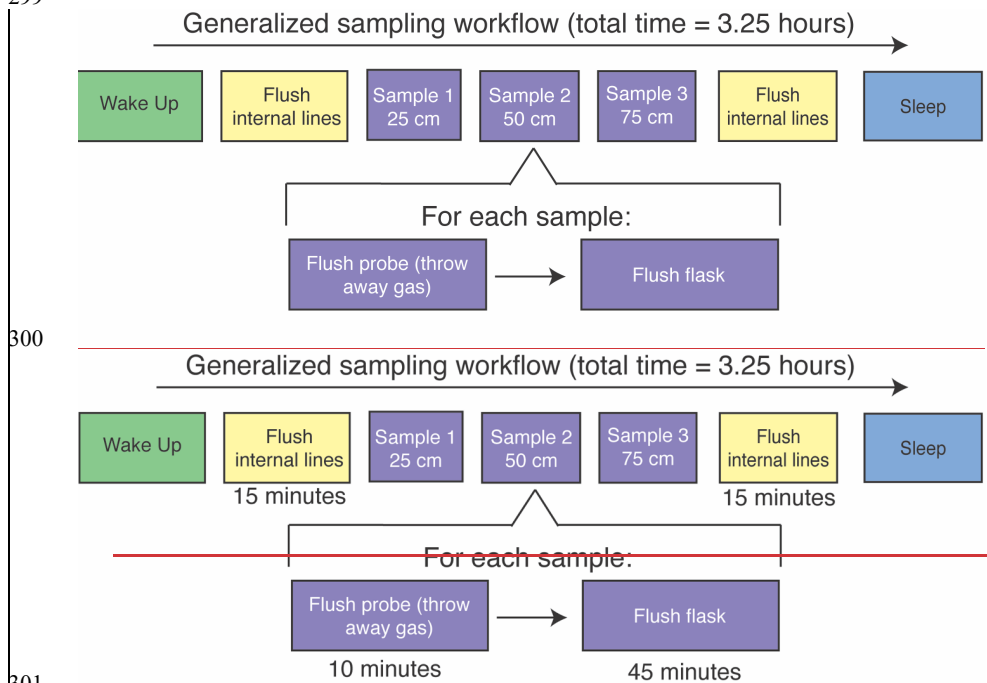
301
302 **Figure 2.** Flow chart of the instrument schedule used for sampling during all field experiments.
303
304 **Table 1.** Description of soil water sampling steps
305

Code Step	Wake-up	Flush internal lines	Flush depth 1	Sample depth 1	Flush depth 2	Sample depth 2	Flush depth 3	Sample depth 3	Flush internal lines	sleep

time (minutes)	1	15	10	45	10	45	10	45	15	1
Valco valve position	flask bypass	flask bypass	flask bypass	2, 5, 8,11, or 14	flask bypass	3, 6, 9, 12, or 15	flask bypass	4, 7, 10, 13, or 16	flask bypass	flask bypass
solenoid valve position	none	soil bypass	25 cm	25 cm	50 cm	50 cm	75 cm	75 cm	soil bypass	none

306 ~~Table 1. Description of soil water sampling steps~~

307

308 ~~probes; and (6) a power relay used to power the Valco valve and mass flow controller. All parts~~
309 ~~are described in detail in Supplemental Table 2.~~

310   In a remote setting, the SWISS units are powered using the combination of a 12 volt~~V~~
311 deep-cycle battery ~~and~~with a 12VDC, 100 watt~~W~~ solar panel that is used to charge the battery.
312 The solar panel is mounted to a piece of plywood that covers the hole where the SWISS is
313 deployed (note, the hole is uncovered in Fig. 1B for illustrative purposes). We opted for this
314 setup because the underground storage of all parts of the system creates a discreet field site that
315 attracts minimal attention from other land users, and helps reduce exposure to temperature and
316 precipitation extremes. In the field, we used a 12VDC-120VAC power inverter to provide simple
317 plug and play power for the Valco valve and mass flow controller. This simple combination was
318 suitable for summertime in the Western U.S. where there are ~~a great number of sunny~~many hours
319 of direct sunlight, and the solar panel was able to easily charge the 12V battery. This setup may
320 need to be adjusted based on location and desired sampling time. Like the automation system,
321 there are many commercial options available for products, and they can be easily adjusted for
322 users' needs; example parts are described in detail in Supplemental Table 2. We also note that in
323 areas where it is possible to plug into a power grid, the deep cycle battery, solar panel and power
324 inverter can be removed.

325

326

4. Methods

We completed all water vapor isotope analyses in the Stable Isotope Lab at the Institute of Arctic and Alpine Research (INSTAAR SIL) at the University of Colorado Boulder between October 2020 and August 2022. ~~In our case,~~ We~~e~~ used a Picarro L-2130*i* water isotope analyzer (Picarro, Inc. Santa Clara, CA) to measure both water concentration and the oxygen and hydrogen isotope ratios of the ~~soil~~ water vapor.

4.1 QA/QC: Testing the SWISS under lab conditions

Our~~The~~ highest order concern for the SWISS is that it remains leak-free, because ~~any~~ leaks would introduce the potential for fractionation or mixing of atmosphere that would alter the stable isotope ratio of the water vapor in the flask. ~~So~~To mitigate leaks, we developed a three-part quality assurance and quality control (QA/QC) procedure that must be completed for each new SWISS prior to the first deployment. The first step detects any ~~significant~~ large, fast leaks using helium detection methods; the second step detects medium scale leaks using~~is to perform a~~ dry air ~~test to detect medium scale leaks~~; and the third step detects slow, small scale leaks using ~~is to perform a~~ water vapor tests~~ to detect slow leaks~~. ~~Below, we quickly summarize each of these QA/QC steps.~~ Full procedural descriptions are available in the supplementary~~l~~ material and the data processing code is available via G~~g~~itH~~h~~ub.

4.1.1 Step 1: Use~~using~~ helium to detect large, *fast* ~~scale~~ leaks

After initial assembly of the SWISS ~~units~~plumbing, we looked for large leaks from the cracking of inlet or outlet tubes on the glass flasks that occasionally occurred while tightening the Swagelok fittings. To do this, we filled the flasks with helium and used a helium leak detector (Leak Detector, Catalog #22655, Restek, Bellefonte, PA, USA)~~to find large leaks~~. ~~Typically, the kinds of leaks we were able to detect with this method were due to cracking of the inlet or outlet on the glass flask that occured while tightening the swagelok fittings.~~ Another easy alternative to a helium leak test~~,~~ is to complete a very short dry air test (methods described below) where the hold-time is on the order of ~~that requires on the order of~~ 12-24 hours.

4.1.2 Step 2: Use dry air to tests~~ detect~~ medium scale leaks

~~Once we felt sure that there were no major leaks in our systems, we completed a dry air test.~~ The goal of this test was to catch any second order, medium-scale leaks associated with either Valco valve fittings or Swagelok fittings that were under tightened. ~~. Typically, this test found swagelok fittings that had been under tightened. The advantage of this kind of test is that it is easy and quick to complete.~~

Step 2A: Fill flasks with dry air

To start every experiment, we filled flasks ~~This test started with a dry air fill. A dry air fill consists of flushing flasks~~ with air that is filtered through D~~d~~rierite (which has a water vapor mole fraction of less than 500 ppm), at 2 L/min for 5 minutes. With a flask volume of 650 ml, this means the volume of the flask is turned over 15 times.

Step 2B: Hold period

370   Flasks were then sealed and left to sit for seven days. This time period can be adjusted by
371 other users to fit their climate or needsassembly.
372
373 *Step 2C: Measure water vapor mole fraction using dead-end pull sample introduction*
374   At the end of the seven-day period, we measured each flask using a the dead-end pull
375 sample introduction (note, italicized terms are specific methods, and are explained in greater
376 detail in supplementary material) method on a Picarro L2130-*i* Isotope and Gas Concentration
377 Analyzer. For this sample introduction method, the inlet to the Vvalco valve was sealed with a
378 1/4 inch ¼" Sswagelok cap and there was no introduction of a carrier gas. As a result, air was
379 removed from the flask based on the flow rate of the Picarro CRDS analyzer (typically 27 - 31
380 ml/min). Flasks were measured for five minutes, which resulteds in ~150 ml of air being
381 removed from the flasks. All components within the SWISS are capable of being fully
382 evacuated. Water vapor mole fractions determined by Picarros are not standardized, so it is impossible to know
383 for sure the exact magnitude of water vapor mole fraction change between the input analysis and the final value at
384 the end of the dry air test. However, these instruments are remarkably stable over weeks, and so the relative changes
385 observed (e.g. increase or decrease of mole fraction relative to the initial amount) are likely reliable, particularly for
386 the larger magnitude changes.
387   isotope wereIf a flask had a water vapor mole fraction of less than 500 ppm, it "passed"
388 step 2 of QA/QC.
389   If a flask had a water vapor mole fraction greater than 500 ppm, it "failed" step 2 of
390 QA/QC, and we tightened both the Swagelok connections on the flasks as well as the fittings
391 between the stainless steel tubing and the Valco valve. We found that in a low-humidity
392 environment, we needed a week to really see leaks, but this timescale would likely be shorter in
393 more humid locations. Additionally, this test could be modified based on available equipment
394 (for example, if an instrument is available to measure trace atmospheric gases, that could be used
395 instead). To ensure that SWISS units continue to operate as expected, this test should be done
396 between field deployments on every SWISS unit.
397   We repeated dry air tests on aany given SWISS unit until the majority (typically at least
398 13/15) of the flasks had a passed step 2 of QA/QC. water vapor mole fraction value of less than
399 500 ppm at the end of the seven day experiment. Water vapor values from the CRDS have not
400 been independently calibrated, but relative variations are believed to be reliable.
401
402 *4.1.3 Step 3: Water vapor tests detect small scale leaks*
403   The purpose of this experiment was to mimic storage of water vapor at concentrations
404 similar to what we might expect in a soil, and for durations similar to those of our field
405 experiments. These testsexperiments were meant to test demonstrate thatwhether during field
406 experiments, flasks filled early in the sampling sequence during field deployments do not leak by
407 the time samples are returned to the lab for measurement. Additionally, these tests were used to
408 demonstrate that flasks that were filled early in the sampling sequence did not lead by the time
409 the samples were returned to the lab for measurement. For this experiment, we filled flasks were
410 filled with water vapor of known isotopic composition and water vapor mole fractionknown
411 concentration, sealed the flasks for 14 days, and then we measured the water vapor concentration
412 mole fraction and isotope values of each flask. We performed 11 water vapor tests that were
413 done across three analytical sessions using six different SWISS units. Across these three
414 sessions, we measured 164 flasks both at the start of the 14-day experiment, and at the end. .
415
416 *Step 3A: Flush flasks with dry air*

417   Prior to putting any water vapor into the flasks (either in the field or in the lab), we
418   completed a dry air fill (as ~~defined~~ described in QA/QC step 2A~~above~~) that served to purge the
419   flasks of any prior water vapor that might exchange with the new sample.
420
421   *Step 3B: Fill flasks with water vapor and measure input isotope values*
422   To supply water vapor to the flasks, we used the vapor permeable ~~tubing~~ probes that were
423   constructed identically to those deployed in the field. We immersed the probes up to the
424   connection between the vapor permeable and impermeable tubing in~~in~~ water, taking care to not
425   submerge the connection point and inadvertently allow~~ing~~ liquid water to enter the inside of the
426   vapor permeable tubing. We flushed the flasks at a rate of 150 ml/min for 30 minutes, and
427   measured the $\delta^{18}O$ and δ^2H values and mole fraction of water vapor as each flask was filled. To
428   fill 15 flasks sequentially, the probes were submerged in water for approximately 7.5 hours.
429   Across three different ~~measurement~~ sessions, we used three different waters that are ~~used~~
430   ~~as~~ tertiary standards in the INSTAAR SIL ~~lab~~ to complete these experiments: a light water made
431   from melting and filtering Rocky Mountain snow ~~(~~(~ -25.5‰ and -187.5‰ VSMOW, for $\delta^{18}O$
432   and δ^2H, respectively), an intermediate water that is deionized (DI) water from the University of
433   Colorado Boulder Campus (~ -16.2‰ and -120.7‰ VSMOW for $\delta^{18}O$ and δ^2H, respectively)
434   and a heavy water that is filtered water sourced from Florida, USA (~ -0.8‰ and -2.8‰
435   VSMOW for $\delta^{18}O$ and δ^2H, respectively). All ~~secondary~~ tertiary lab standards are characterized
436   relative to international primary standards obtained from the International Atomic Energy
437   Agency and are reported relative to the V-SMOW/SLAP standard isotope scale. ~~We flushed the~~
438   ~~flasks at a rate of 150 ml/min for 30 minutes, and measured the $\delta^{18}O$ and δ^2H values and mole~~
439   ~~fraction of water vapor as each flask was filled.~~ To calculate the input value, we averaged $\delta^{18}O$
440   and δ^2H values over the last three minutes of the filling period.
441   ~~Then, w~~We then stored the water vapor in the flasks for 14 days. At the end of the 14-day
442   storage period, we measured each flask to evaluate if the ~~isotope composition~~$\delta^{18}O$ and δ^2H
443   values had significantly changed over the storage period.
444
445   *Step 3C: Measure the water vapor isotope values*
446   ~~At the end of the 14-day storage period, we measured each flask to evaluate if the isotope~~
447   ~~composition had significantly changed over the storage period.~~ To mitigate memory effects
448   between flasks, we ran dry air via the flask bypass loop (port one~~1~~ of every ~~Valco valve~~SWISS
449   unit) for five~~5~~ minutes between each flask measurement. To verify that the impermeable tubing
450   between the SWISS and the Picarro was sufficiently dried, we waited until the water vapor
451   mixing ratio being measured by the Picarro was below 500 ppm for >30 seconds.
452   During this ~~5 minute~~five-minute window, we used a heat gun to manually warm each
453   flask. ~~The purpose of the heating was to help create a longer, more stable window of~~
454   ~~measurement time.~~ We believe heating the flasks creates a more stable measurement by limiting
455   water vapor bound to the glass walls of the flask and by helping to homogenize the water vapor
456   within the flask. While we did not strictly control or regulate the temperature of the flask~~s was~~
457   ~~not strictly controlled or regulated~~, they were all warm to the touch.
458   Once we warmed the flask ~~was warmed~~ and dried the impermeable tubing~~dried~~, water
459   vapor was introduced to the CRDS using one of two methods: 1) the dead-end pull sample
460   introduction method described above, or 2) a *dry air carrier gas sample introduction* method.
461   During the dry air carrier gas sample introduction method, dry air is continuously flowing
462   through the flask at a rate of 27-31 ml/min for the entire 12-minute measurement period. To

reach a water vapor mole fraction of approximately 25,000 ppm (the optimal humidity range for the Picarro L2130-*i*), we diluted the water vapor with dry air at a rate of 10 ml/min. Without dilution, the concentration out of the flasks is as high as 35,000 - 40,000 ppm, which leads to linearity effects on a Picarro L2130-*i* that can be challenging to correct for. The dead-end pull method is preferable when the water vapor mole fraction inside the flask is low (<17,000 ppm), because there is no additional introduction of dry air. The introduction of dry air decreases the water vapor mole fraction throughout the measurement, and in fairly dry flasks, using the dry air carrier gas method~~,~~ can lower the water vapor mole fraction to below 10,000 ppm. Below 10,000 ppm, there are large linearity isotope effects associated with the measurement on a Picarro L2130-*i*, and the isotope values are challenging to correct into a known reference frame, just as with high water vapor mole fractions. ~~. But, t~~The major downside of the dead-end pull method is that condensation is more likely to ~~can~~ forms in the stainless steel tubing that connects the flasks to the Valco valve, as well as the Valco valve itself, ~~far more commonly as compared~~than ~~to~~compared to the dry air carrier gas method. ~~During the dry air carrier gas method, dry air is continuously flowing through the flask at a rate of 27-31 ml/min for the entire 12 minute measurement period. Additionally, to reach a water vapor mole fraction of approximately 25,000 ppm (the optimal humidity range for the CRDS Picarro L2130-i), we diluted the water vapor with dry air at a rate of 10 ml/min. Without dilution, the concentration out of the flasks is as high as 35,000 - 40,000 ppm, which leads , as happens under low water vapor mole fractions,The dry air to saturation issues on a Picarro L2130-i. Providing a~~ carrier gas method prevents condensation from forming in the Valco valve and tubing, and prevents fractionation that may occur because of changing pressure within the flask. It is possible that during a dead-end pull on the flask, ~~that~~ heavier isotopes may remain attached to the walls of the flask, coming off later as the pressure drops.~~.~~ For these~~is~~ reasons, ~~T~~the dry air carrier gas sample introduction method is our preferred method for sample introduction in most cases.

For each flask, we looked at the stability of the isotope values as well as either a stable water vapor mole fraction if the dead end pull method was being used or a steady, linear decrease in water vapor mole fraction if the dry air carrier gas method was being used.~~we looked at signal stability individually, and~~ F~~f~~or approximately 90% of the flasks we found that after excluding the first three minutes of measurement of each flask, the subsequent three minutes were the most stable~~and consistent~~. For the remaining ~10% of the flasks, using a time window that started either ~30 seconds earlier or ~30 seconds later to create an average isotope value offered a more stable isotope signal with smaller instrumental uncertainties. ~~For some flasks, using either a later portion of the measurement period, or slightly earlier offered a more stable signal.~~ Any flask that ~~would benefit from~~required specialized~~individual~~ treatment during the data reduction process was flagged during measurement.

Step 3D: Data correction
During these experiments, we monitored instrument performance (e.g.~~i.e.~~ drift) ~~and stability were monitored~~ in two ways. First, to run standards identically to how samples were collected, we introduced tertiary standards, described above, using vapor probes. The water vapor produced by the vapor permeable probes was flushed through the SWISS unit via the flask bypass loop and diluted with a 10 ml/min dry air flow to reach a water vapor mole fraction of approximately 25,000 ppm before entering the Picarro. Second, we introduced ~~using~~ a suite of four secondary standards that have been calibrated against primary standards, and reported against VSMOW/SLAP ~~four waters of known composition via~~that were introduced to the CRDS

509 ~~using~~ a flash evaporator system~~,~~ described in detail by Rozmiarek and others (2021). Th~~is~~e flash
510 evaporator system ~~described by Rozmiarek and others (2021)~~ can be used to adjust the water
511 vapor mole fraction to create linearity corrections at high and low water vapor mole fractions.
512 ~~Additionally, instrument stability was assessed by measuring water vapor of known composition~~
513 ~~that was produced using the vapor probes, in a fashion that is identical to how the flasks were~~
514 ~~flushed.~~
515 After correcting data into a common reference frame, we calculated the difference
516 between the input isotope values and the ending isotope values.
517 The results of these tests were used to carefully document flasks that do not perform well,
518 and any idiosyncrasies of SWISS units. That way, during field deployment suspicious those
519 flasks could be easily identified and investigated.
520
521 **4.2 Field suitability ~~and Field application~~ experiments:**
522 *4.2.1 Field suitability experiment #1: Long term field ~~leak~~ dry air test*
523 As a complement to the QA/QC we did under lab conditions, we also completed long
524 term dry air tests at our field sites. ~~Th~~We had three goals associated with these experiments. The
525 first ~~e purpose of these experiments~~ was to ~~demonstrate that~~test whether, even under field
526 conditions, where daily temperature and relative humidity fluctuations are different than in a lab
527 setting, the flasks ~~a~~were still resistant to atmospheric intrusion. ~~Furthermore,~~Second, we used
528 th~~ese is leak~~ tests ~~was used~~ to ~~demonstrate that~~evaluate whether the flasks that we~~are~~ flushed
529 with soil water vapor near the end of a sampling sequence ~~do not take~~took on ~~an~~ atmospher~~ic~~e
530 ~~isotope composition~~ prior to sampling. Lastly, we chose these time intervals because they
531 bracket the typical length of a deployment, which helped us determine how quickly flasks should
532 be measured after bringing a SWISS back to the lab.
533 ~~filled last during the sampling sequence had not taken on an atmospheric isotope~~
534 ~~composition prior to sampling.~~
535 Like all field deployments, we started with a dry air fill, and then one SWISS unit was deployed
536 to each of our three field sites. No soil water was collected during these deployments. The
537 duration between filling the flasks with dry air to measuring the flasks was ~~anywhere~~ between 34
538 - 52 days. The 34 and 52 day tests were~~as~~ done during June 2022 and August 2021, respectively,
539 and therefore tests the SWISS under warm summertime conditions. The 43 day test was done in
540 October 2021, which included nights where air temperatures fell below 0°C. ~~Though the SWISS~~
541 ~~is not directly exposed to the air in its deployment hole, t~~The only barrier between air and the
542 SWISS in its deployment hole was~~is onl~~ a plywood board, and so this deployment tested the
543 suitability of the SWISS to maintain integrity under freezing conditions. ~~The 52 day test was~~
544 ~~done in August 2021 and also tests the SWISS under warm, summertime conditions~~
545
546
547 *4.2.2. Field suitability experiment #2: Mock field tests*
548 To ~~demonstrate that~~test whether the automation code and sampling scheme we
549 ~~proposed~~developed worked as expected on short, observable timescales, we set up an experiment
550 to simulate field deployment of one SWISS unit (Meringue) near the University of Colorado
551 Boulder. This test ~~used~~ applied the automation components and remote power setup described in
552 the materials section. During this field-simulation experiment, our goal was to collect three
553 discrete samples each sampling period, to simulate the collection of ~~samples~~ water vapor from
554 three soil depths. An important goal of this test was to ~~at each field site. Importantly, we wanted~~

555 ~~to demonstrate that~~test whether the sampling scheme ~~does not~~ introduce~~d~~ ~~significant~~any memory
556 effects between samples. We followed the sampling protocol described in figure 2 and table 1.
557   The day before the experiment began, all flasks were flushed with dry air as described in
558 section 4.1.2. Over the course of 25 hours, all 15 flasks were filled with three different vapors
559 according to a set schedule as would be done in the field. Two of the vapors were created by
560 immersing the water vapor permeable probes in the
561 ~~were water vapors, created from the~~ light water and intermediate water as described ~~above~~ in
562 section 4.1.3~~the water vapor test section~~. The third was water vapor from the ambient
563 atmosphere. All three vapors were sampled using vapor permeable probes constructed identically
564 to those deployed in the field. For this experiment, we filled three flasks per cycle with each one
565 of the waters (e.g. Flask 2 = light, Flask 3 = intermediate, Flask 4 = ~~a~~Atmosphere). The choice to
566 sample atmosphere alongside two waters reflects our second goal of this test, which was to
567 demonstrate that sampled water vapor isotope values do not drift towards atmospheric values
568 (Magh et al., 2022).
569   Following the sampling schedule, we stored the SWISS unit
570 ~~For seven days, the SWISS unit was stored i~~in a simulated field setting for seven days. ~~, while~~
571 ~~the water vapor remained in the flasks.~~ At the end of the seven days, we measured the flasks. For
572 flasks that had a high water vapor mole fraction (i.e. ~~flasks with a higher water vapor mole~~
573 ~~fraction (~~light and intermediate water vapor samples) we used the dry air carrier gas sample
574 introduction method ~~were measured using the carrier gas sample introduction method~~. For flasks
575 that had a ~~, whereas those with a~~ low water vapor mole fraction (i.e. atmosphere, ~15,000 ppm)
576 we used the ~~were measured using the~~ dead end pull sample introduction method.
577
578   To create average values for each flask, we followed the same averaging protocol
579 described in section 4.1.3. We used equations 2A and 2B from Rothfuss et al., (2013) to convert
580 from water vapor to liquid values. Then, using secondary and tertiary standards, data were
581 corrected into the VSMOW ~~data frame~~isotope scale. Finally, the SWISS unit offset correction
582 (detailed below in section 6.1.2) was applied.
583
584 *4.~~2~~.3 ~~Full field deployment experiment~~Example Field Deployment: One month period*
585   We deployed one SWISS unit each to the three field sites described in summer 2022.
586 Before deployment, all SWISS units were flushed with dry air following the protocol outlined in
587 section 4.1.2. Flasks were flushed with dry air one to three days prior to field deployment.
588   At each site, w~~W~~e sampled at three depths (25 cm, 50 cm, and 75cm) on each sampling
589 day, following the protocol described in figure 2 and table 1. We sampled ~~at each depth every 5~~
590 ~~days~~soil water from all three depths every five days (protocol length = 25 days total). At Oglala
591 National Grassland, s~~S~~amples were taken every five days from 2022-06-25 to 2022-07-14. At
592 the Briggsdale, CO site s~~S~~amples were taken every five days between 2022-07-17 and 2022-08-
593 06. At the Seibert, CO site, s~~S~~amples were collected every five days between 2022-06-19 and
594 2022-07-04.
595   At the end of a 28- day period, the SWISS units were returned to the lab, and measured.
596 SWISS units were measured within five days of returning from the field. The maximum number
597 of days a flask held sample water vapor during these deployments was 32 days. The
598 measurement protocol and data ~~reduction~~ averaging protocol follows the procedures described in
599 ~~the water vapor QA/QC test section above~~section 4.1.3. The data correction scheme follows as in
600 the section ~~above~~4.2.2.

5 Results

5.1 QA/QC Results

5.1.1 Dry air test

Figure 3 shows the results of a seven-day dry air test for three SWISS units (marked by the ~~box~~ unit name) (SI Table 3). For all three SWISS units, at least 13/15 of the flasks maintained a water vapor mole fraction value of less than 500 ppm over the seven-day period. In two of the three SWISS units (Lindt and Raclette), the water vapor mole fraction for flasks was randomly distributed around approximately 350 ppm. In Toblerone there was a systematic decrease in water vapor mole fraction from flask ~~two~~2 through flask 16, matching the order in which the flasks were filled with dry air initially. In ~~both~~ all three ~~Lindt and Toblerone~~SWISS units, flask ~~two~~2 had the highest water vapor mole fraction of all the flasks. Supplemental figure 2 shows the results of successive dry air tests on the SWISS unit Toblerone where Swagelok fittings were tightened between tests. There was a significant decrease in measured water vapor mole fraction for many flasks, but particularly for flasks 10 and 11 as a result of tightening the fittings.
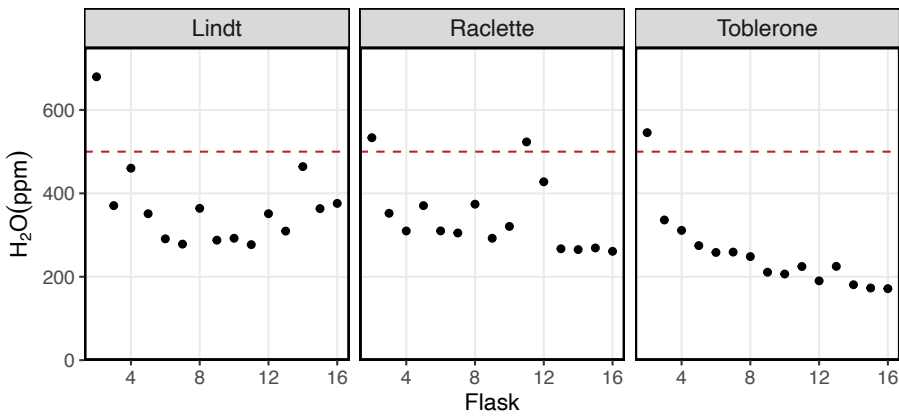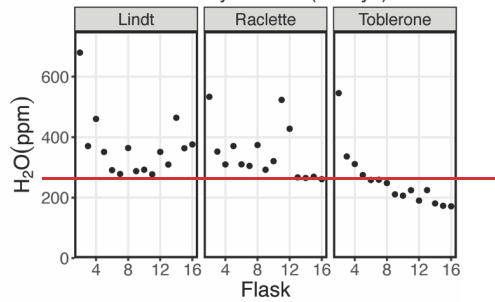
Figure 3. Results of a dry air test from three different SWISS units named: Lindt, Raclette and Toblerone. The majority of the flasks maintain a water vapor mixing ratio of less than 500 ppm.

5.1.2. Water vapor test

In panels a and b of figures 4 and 5, we show the results of 11 different water vapor tests performed across three analytical sessions using 6 different SWISS units. This dataset includes water vapor tests using three different water vapors (light, intermediate and heavy) and uses both the dead-end pull and dry-air carrier gas methods to introduce water vapor to the CRDS. Across these three sessions, we measured 164 flasks while filling them with water vapor and at the end of the two week hold period. After correcting for instrument drift, we calculated the difference between the starting and end values to assess drift in water vapor isotope values due to leaking or other measurement bias.

Figure 4 shows the $\delta^{18}O$ results of 11 water vapor tests performed using six different SWISS units. Ideally, we expect a normal distribution centered about 0 within the uncertainty limits of the water vapor probes (Oerter et al., 2016). For $\delta^{18}O$, the mean difference between the start and end values for the flasks is 1.1‰ with a standard deviation of 0.72‰ (outliers removed). There is a consistent positive offset, with a few clear outliers (Fig. 4A). We do not observe a consistent difference between water vapor sample introduction methods (~~Supp~~Supplemental. Fig. 3~~2~~). After removing outliers (< Q1 - 1.5*IQR or > Q3 + 1.5*IQR, n = 15) ~~from the dataset~~, we compared the kernel density estimate shape to a normal distribution calculated from the mean and standard deviation of the dataset to assess dataset normality (Fig. 4B). A normal distribution slightly overestimates the center of the data, but captures the overall shape fairly well. Therefore, we used the median offset (1.0‰) to correct our water vapor isotope values, and used the interquartile range of the dataset (outliers removed) to estimate uncertainty of the SWISS as ± 0.9‰ . In figure 5C, for simplicity, we just present the results from 45 flasks (three SWISS units), with the 1.0‰ offset correction applied. After correction, data are randomly distributed about 0, and are within the uncertainty range of ± 0.9‰ (Supp. Table 4).

Figure 5 shows the δ^2H results of 11 water vapor tests. For δ^2H, the mean difference between the start and end values is 2.63‰ with a standard deviation of 2.85‰ (outliers removed). Similar~~ly,~~ to $\delta^{18}O$, we ~~ideally~~ expected a normal distribution of differences centered around 0. As with $\delta^{18}O$, there was a consistent positive offset with some outliers (~~i.e.~~i.e., < Q1 - 1.5*IQR or > Q3 + 1.5*IQR) (Fig. 5A). After removing outliers (n = 26) ~~from the dataset~~, we compared the kernel density estimate to a normal distribution calculated from the mean and standard deviation of the dataset to assess dataset normality (Fig. 5B). As ~~for~~with $\delta^{18}O$, the center of the dataset is overestimated by the mean, but the overall peak shape is roughly captured. We therefore use the median value of 2.3‰ as an offset correction~~,~~ and estimate uncertainty at ±3.7‰ for δ^2H from the interquartile range. In figure 5C, we present the results from 45 flasks (three SWISS units), with the 2.3‰ offset correction applied. Data are randomly distributed about ~~0, and~~0 and are within the uncertainty range of ± 3.7‰ (~~Supp~~Supplemental. Table 4).

When we compared the results in figures 4C and 5C, we found that flasks that performed adequately ~~in oxygen isotope space~~for $\delta^{18}O$ ~~d18O~~did not always perform adequately ~~in hydrogen isotope space~~for δ^2H~~d2H~~. The results from the SWISS unit Lindt display this ~~trend~~behavior particularly well. Less commonly, some flasks that were within uncertainty of the system for ~~hydrogen isotope values~~ δ^2H~~d2H~~ were not within uncertainty of the system ~~in oxygen isotope values~~for $\delta^{18}O$~~d18O~~, like flask 8 in the SWISS unit Toblerone (Figs. 4C, 5C). In a dual isotope

plot, there is a strong positive correlation between δ^2H and $\delta^{18}O$ with a slope of 3.14 and an R^2 value of 0.62 (Supplemental Fig. 4).

5.2 Field suitability and field deployment experiment results

5.2.1. Dry air test

Figure 6A shows the result of placing SWISS units that were flushed with dry air out into field conditions over the course of 34 – 52 days (SI Table 3). We chose these time intervals because they bracket the typical length of a deployment, which helped us determine how quickly flasks should be measured after bringing a SWISS back to the lab. At the timescale of 34 – 43 days, 13 of the 15 flasks typically maintained a water vapor mole fraction of less than 1000 ppm. At the timescale of 52 days, eight of the 15 flasks had a water vapor mole fraction between 1000 – 2500 ppm, and the remaining seven flasks had a water vapor mole fraction of less than 1000 ppm. Given that these tests were completed with different SWISS units, these data also include some of the inter-unit variability.

681
682

684
685
686 **Figure 4.** ~~d18δ^{18}O O R~~results of the water vapor tests. A) Boxplot of the difference between the starting
687 δ^{18}O value and the final δ^{18}O value of all 164 flasks. B) After removing the outliers from the dataset, the
688 kernel density estimate (black line) and the normal distribution calculated from the dataset (dashed green)
689 are shown. C) After applying the offset correction of 1.0‰, the difference between the starting δ^{18}O value
690 and the final δ^{18}O value for three boxes from the August 2022 session are shown. An uncertainty of ±
691 0.9‰ is marked with a dashed line, and data points that fall outside that uncertainty are colored red.
692
693
694
695
696
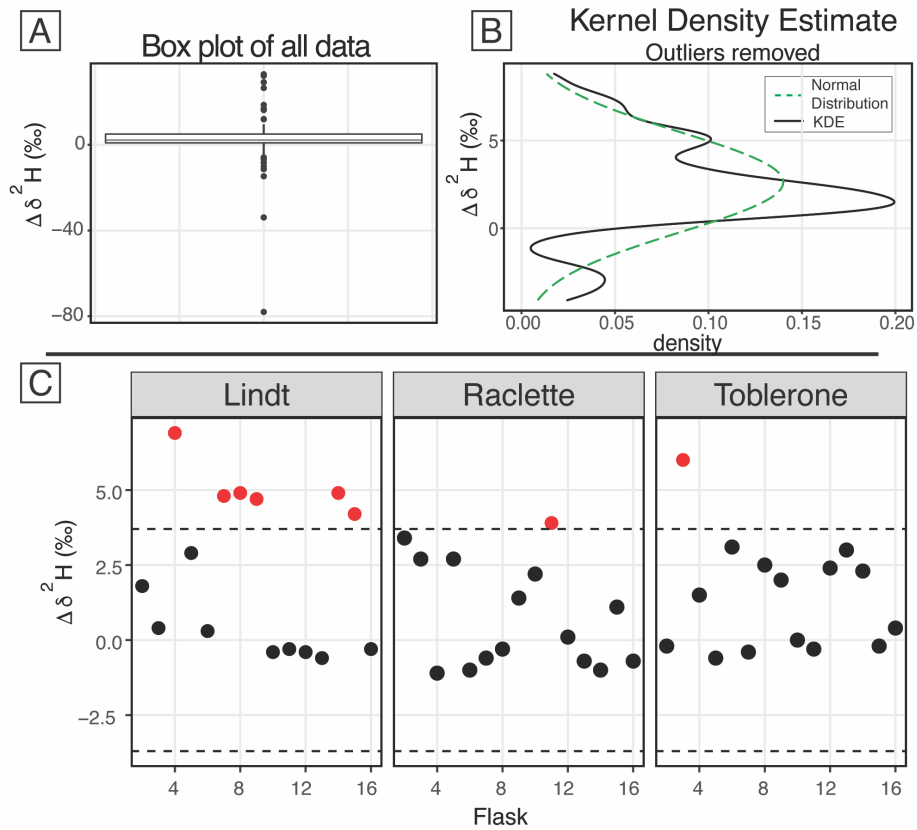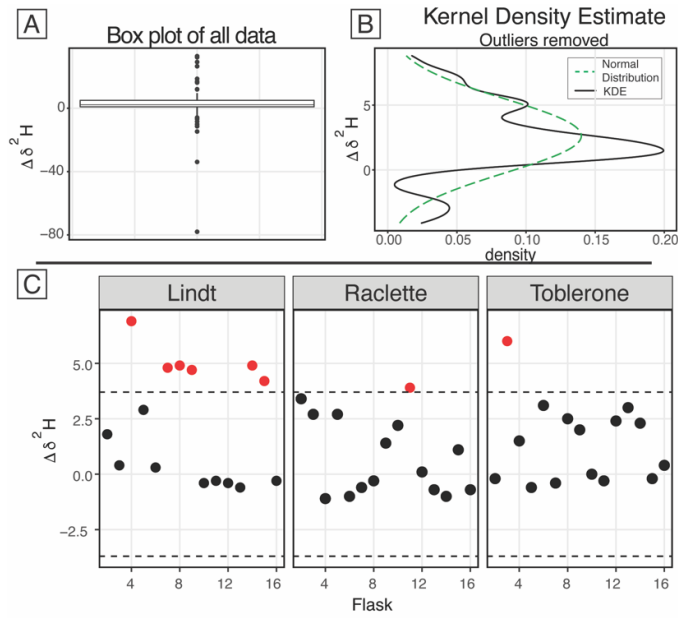
Figure 5. δ^2H ~~Rd2H~~ results of the water vapor tests A) Boxplot of the difference between the starting δ^2H value and the final δ^2H value of all 164 flasks. B) After removing the outliers from the dataset, the kernel density estimate (black line) and the normal distribution calculated from the dataset (dashed green) are shown. C) The difference between the starting δ^2H value and the final δ^2H value for three boxes from the August 2022 session are shown after applying the offset correction of 2.3‰. An uncertainty of ± 3.7‰ is marked with a dashed line, and data points that fall outside that uncertainty are colored red.

5.2 Field suitability test ~~and field deployment experiment~~ results

5.2.1 Dry air test

Figure 6A shows the result of placing three different SWISS units~~,~~ that were flushed with dry air~~,~~ out into the field ~~conditions over the course of~~for 34 - 52 days (SI Table 3). This timescale (4-6 weeks) is similar to most field deployments. ~~We chose these time intervals because they bracket the typical length of a deployment, which helped us determine how quickly flasks should be measured after bringing a SWISS back to the lab.~~ At the timescale of 34 - 43 days, 13 of the 15 flasks typically maintained a water vapor mole fraction of less than 1000 ppm. ~~At the timescale of 52 days, eight of the 15 flasks had a water vapor mole fraction between 1000 - 2500 ppm, and the remaining seven flasks had a water vapor mole fraction of less than 1000 ppm. Given that these tests were completed with different SWISS units, these data also include some of the inter-unit variability.~~ Over the 52 days, seven flasks maintained a water vapor mole fraction less than 1000 ppm and the remaining 8 had a water vapor mole fraction between 1000 - 2500 ppm.

5.2.2 Automation test

Figure 6B shows the results of using the automation code to collect and store water vapor of known composition for seven days (Table 2). In both plots, the known values of the water are shown as a long-dash line. Uncertainty on those measurements is estimated at ±0.5‰ and ±2.4‰ for $\delta^{18}O$ and δ^2H, respectively (Oerter et al., 2016), shown as the dotted lines. We estimated the isotope value of the atmosphere at the time of sampling with water vapor mole fraction, $\delta^{18}O$, and δ^2H data from the CRDS in the lab. The isotope value, that was corrected as described in section 4.2.2, of each flask is shown, with uncertainty associated with the SWISS units estimated at ±0.9‰ and ±3.7‰ for $\delta^{18}O$ and δ^2H, respectively.

Seven of the nine flasks filled with flash-evaporated water vapor overlap within uncertainty of the known $\delta^{18}O$ value for those standards (top plot, Fig. 6B), and four of the five flasks filled with atmospheric vapor overlap within uncertainty of our estimated $\delta^{18}O$ value. Flasks that fall outside of the bounds of uncertainty have lower $\delta^{18}O$ values than the expected value. For δ^2H, (bottom plot, Fig. 6B) only three of the nine flasks filled with flash-evaporated water vapor overlap within uncertainty of the known value of those standards, while four of the five flasks filled with atmospheric vapor overlap within uncertainty of the estimated δ^2H value. Flasks that fall outside of the bounds of uncertainty have higher δ^2H values than the expected value.

763   **Table 2.** Results of the Automation test

SWISS	Flask	water	$\delta^{18}O$ (‰)	δ^2H (‰)
Meringue	2	DI	-14.4	-122.2
Meringue	3	Atmosphere	-10.1	-105.6
Meringue	4	Light	-24.6	-193.7
Meringue	5	DI	-15.0	-130.8
Meringue	6	Atmosphere	-9.4	-103.4
Meringue	7	Light	-25.1	-201.5
Meringue	8	DI	-17.3	-140.5
Meringue	9	Atmosphere	-9.1	-98.4
Meringue	10	Light	-23.7	-200.7
Meringue	11	DI	-14.1	-122.5
Meringue	12	Atmosphere	-8.7	-94.5
Meringue	13	Light	-22.7	-181.2
Meringue	14	DI	-15.2	-120.5
Meringue	15	Atmosphere	-9.2	-101.1
Meringue	16	Light	-23.3	-192.9

764
765
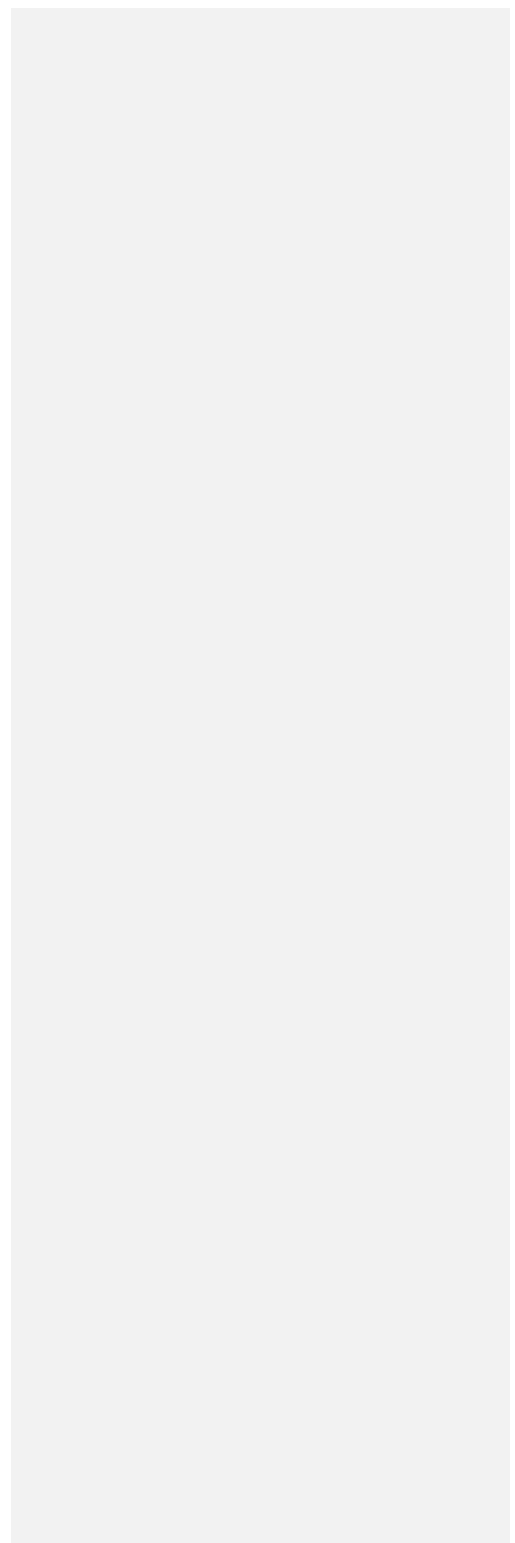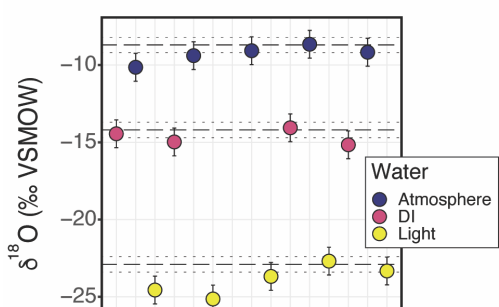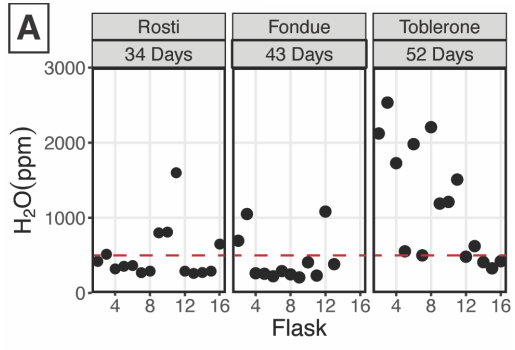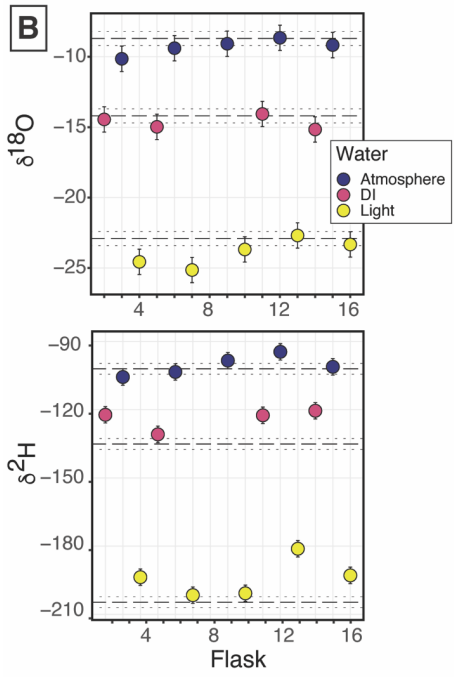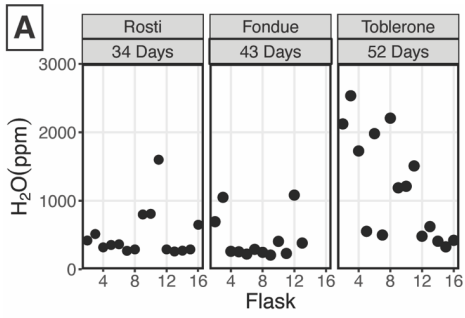
767
768
769
770
771
772
773
774
775
776
777
778
779
780
781
782
783
784
785
786
787
788
789
790
791
792
793
794
795
796
797
798
799
800
801
802
803
804
805
806
807
808 **Figure 6.** A) Results from three different field-based long dry air tests. B) Results from the automation
809 field suitability tests using the SWISS unit named Meringue. Flasks that sampled atmosphere are shown
810 in blue, flasks that sampled deionized water (DI) are shown in pink, and flasks that sampled the light
811 water are shown in yellow. The top plot shows the $\delta^{18}O$ results, and the bottom plot shows the δ^2H results.
812
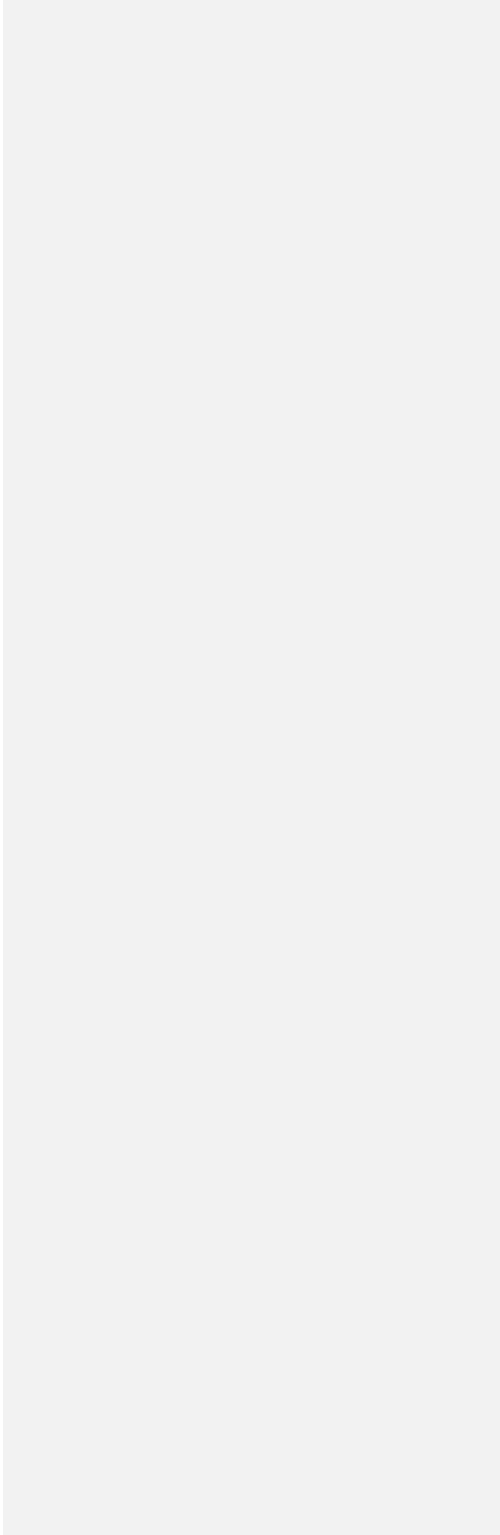
5.2.2. Automation test

Figure 6B shows the result of using the automation code to collect and store water vapor of known composition for seven days (Table 2). In both plots, the known values of the water are shown as a long-dash line. Uncertainty on those measurements is estimated at 0.5‰ and 2.4‰ for $\delta^{18}O$ and δ^2H respectively (Oerter et al., 2016), shown as the dotted lines. We estimated the isotope value of the atmosphere at the time of sampling with data from the CRDS in the lab. The corrected isotope value of each flask is shown, with uncertainty associated with the SWISS units estimated at 0.9‰ and 3.7‰ for $\delta^{18}O$ and δ^2H, respectively.

Seven of the nine flasks filled with water vapor overlap within uncertainty of the known $\delta^{18}O$ value for those standards (top plot, Fig. 6B), and four of the five flasks filled with atmospheric vapor overlap within uncertainty of our estimated $\delta^{18}O$ value. Flasks that fall outside of the bounds of uncertainty tend to have lower $\delta^{18}O$ values than the expected value. For δ^2H, (bottom plot, Fig. 6B) only three of the nine flasks filled with water vapor overlap within uncertainty of the known value of those standards, while four of the five flasks filled with atmospheric vapor overlap within uncertainty of the estimated δ^2H value. Flasks that fall outside of the bounds of uncertainty typically have higher δ^2H values than the expected value.

SWISS	Flask	water	$\delta^{18}O$ (‰)	δ^2H (‰)
Meringue	2	DI	-14.4	-122.2
Meringue	3	Atmosphere	-10.1	-105.6
Meringue	4	Light	-24.6	-193.7
Meringue	5	DI	-15.0	-130.8
Meringue	6	Atmosphere	-9.4	-103.4
Meringue	7	Light	-25.1	-201.5
Meringue	8	DI	-17.3	-140.5
Meringue	9	Atmosphere	-9.1	-98.4
Meringue	10	Light	-23.7	-200.7
Meringue	11	DI	-14.1	-122.5
Meringue	12	Atmosphere	-8.7	-94.5
Meringue	13	Light	-22.7	-181.2
Meringue	14	DI	-15.2	-120.5
Meringue	15	Atmosphere	-9.2	-101.1
Meringue	16	Light	-23.3	-192.9

Table 2. Results of the Automation test

841   ***5.2.3 Example Field deployment results***

842   Figure 7 shows the results from three field deployments in Oglala National Grassland,

843   Nebraska; Briggsdale, Colorado; and Seibert, Colorado (table 3).

844
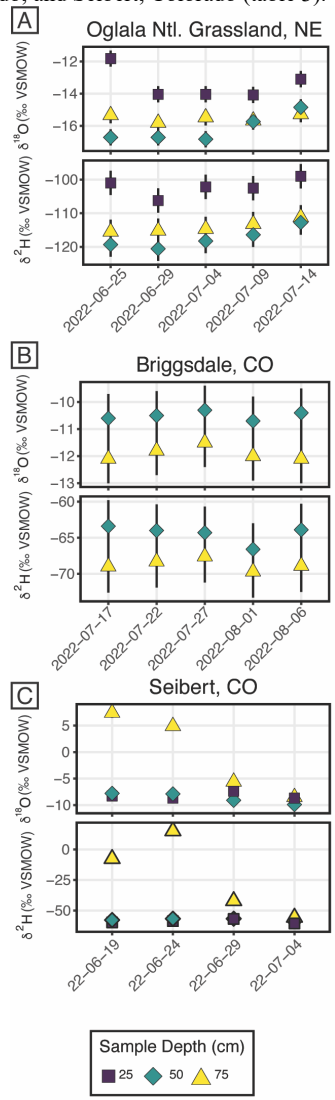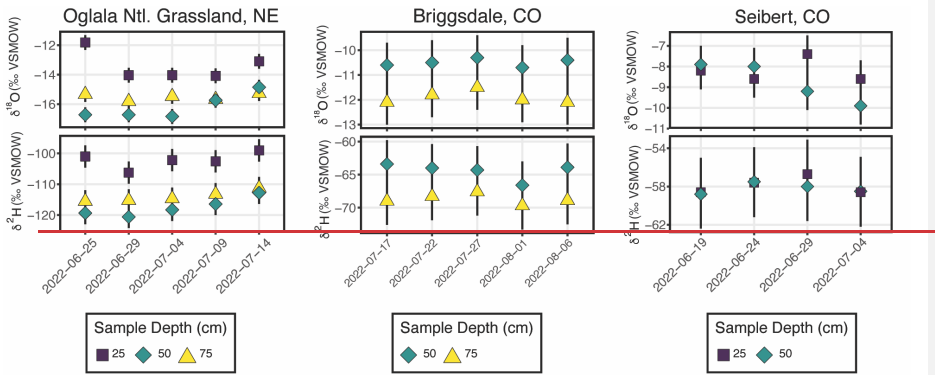
Figure 7. Results from all three field deployments to A) Oglala National Grassland, NE, B) Briggsdale, CO and C) Seibert, CO. Note, the y-axis scale for all three plots is different.

There are 15 samples from Oglala National Grassland (Fig. 7A, Table 3); five from 25 cm depth, five from 50 cm depth and five from 75 cm depth. ~~Samples were taken approximately every five days from 2022-06-25 to 2022-07-14.~~ Four of the five samples from 25 cm overlap within uncertainty in δ^{18}O value, and all five samples overlap with uncertainty in δ^2H value. There is a significant decrease in the δ^{18}O value at 25 cm between 2022-06-25 and 2022-06-29. There is no similar shift in δ^2H value over the same time period. The first three samples from 50 cm overlap in both δ^{18}O and δ^2H values, then the final two samples ~~drift~~shift to higher isotope values. ~~All five samples from 75 cm overlap in δ^{18}O and δ^2H values.~~ Similar to the samples from 50 cm, there is a trend towards higher δ^2H values for the last three samples. All five samples from 75 cm overlap in δ^{18}O and δ^2H values. On a dual isotope plot, data from 50 cm and 75 cm cluster together at lower values, ~~and~~while the ~~Overall,~~ δ^{18}O and δ^2H values from 25 cm are ~~significantly~~ higher ~~(Figs. 7A, 8A)~~than the values from 50 and 75 cm depth. All of the data ~~overalp~~ overlap within uncertainty with the global meteoric water line, except for the 25 cm depth sample from 2022-06-25 (Fig. 8A). The calculated D-excess values ~~all overlap~~are all within uncertainty of~~, and with~~ 10‰ and each other between 2022-06-29 and 2022-07-14 (Fig 8B), except for t~~.~~ The 25 cm depth sample from 2022-06-25, which has a D-excess value of -6.6‰, consistent with evaporative enrichment of soil water at that depth and time. ~~Generally, samples from 50 cm depth have lower δ^{18}O and δ^2H values than samples from 75 cm depth.~~
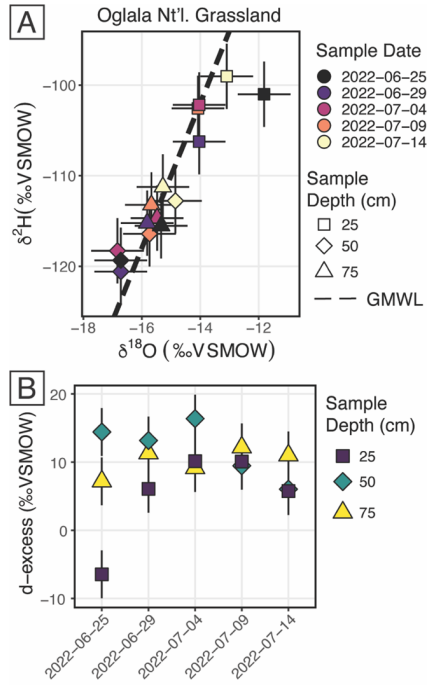
869
870 **Figure 8.** Results from the Oglala National Grassland, NE field site. A) δ^2H vs. δ^{18}O, where the dashed
871 line is the global meteoric water line. The shapes for ~~of~~ the different depths sampled matches figure 7,
872 and the color of the points is the date on which the soil water was sampled B) A plot of d-excess. Note,
873 both the color and shape match figure 7.
874

875   There are 10 samples from Briggsdale, CO (Fig. 7B, Table 3); five samples each ~~are~~
876 from ~~a~~ vapor probes buried at 50 cm ~~depth and five samples are from a vapor probe buried at~~and
877 75 cm depth. Data from 25 cm at Briggsdale, CO were excluded because the water vapor mole
878 fractions from all of the flasks ~~with samples at this depth had~~were extremely low ~~water vapor~~
879 ~~mole fractions~~ (<13,000 ppm). We excluded these data because these samples are associated
880 with a very dry soil (VWC < 0.05), ~~,~~ and ~~so~~ it is not clear how much sampling gas (N_2) is
881 injected into the soil using the vapor permeable tubing under very dry conditions (Quade et al.,
882 2019), and therefore how representative these isotope data are of soil water. Moreover, below
883 13,000 ppm there are large linearity effects on a Picarro L2130-i, and it is ~~very~~ challenging to
884 correct those data if they were measured using the dry-air carrier sample introduction method.
885 ~~*those data may either represent atmosphere or soil gas from an extremely dry soil.* Samples were~~
886 ~~taken every five days between 2022-07-17 and 2022-08-06. A~~While all samples overlap within
887 uncertainty ~~in~~for both $\delta^{18}O$ and δ^2H values, ~~however~~ the absolute values of samples from 50 cm
888 are ~~clearly~~consistently offset to higher values for both $\delta^{18}O$ and δ^2H as compared to samples
889 from 75 cm.
890   There are 128 samples from Seibert, CO (Fig. 7C, Table 3); four ~~samples are from a~~
891 ~~vapor probe buried at 25 cm depth and four samples are from a vapor probe buried at 50 cm~~
892 ~~depth~~from each sampling depth (25, 50 and 75 cm). ~~Samples collected from 75 cm depth at~~
893 ~~Seibert, CO were discarded because there were significant problems with condensation while~~
894 ~~measuring these flasks, and so all data were considered spurious. Samples were collected every~~
895 ~~five days between 2022-06-19 and 2022-07-04.~~ At 25 cm depth, $\delta^{18}O$ values of three of the four
896 samples overlap within uncertainty~~;~~, while the 25 cm sample from 2022-06-29 ~~that does not~~
897 ~~overlap~~ has a higher $\delta^{18}O$ value than the other three samples.~~.~~ At 25 cm depth, δ^2H values
898 overlap within uncertainty for all four samples. At 50 cm depth, there is a steady decrease in
899 $\delta^{18}O$ value over the sampling period, while δ^2H values for all four samples remain steady~~. All~~
900 ~~samples from 50 cm depth~~ and overlap within uncertainty. At 75 cm depth, samples have a very
901 large range of $\delta^{18}O$ values between -8.5‰ and 7.4‰, and δ^2H values range between -55.7‰ and
902 15.1‰. Almost all of the samples from 75 cm depth were associated with condensation in the
903 sample introduction lines during measurement.

904

Table 3. Results from the three field deployments of SWISS.

Site	Date	Sample Depth (cm)	Flask	T (°C)	$\delta^{18}O$ (‰)	$\delta^{18}O$ (‰) Analytical Error	δ^2H (‰)	δ^2H (‰) Analytical Error
Briggsdale	2022-07-17	50	3	25.1	-10.8	0.2	-65.6	0.6
Briggsdale	2022-07-17	75	4	23	-12.1	0.2	-69	0.7
Briggsdale	2022-07-22	50	6	25.9	-10.7	0.3	-67.1	0.7
Briggsdale	2022-07-22	75	7	23.6	-11.9	0.2	-69	0.6
Briggsdale	2022-07-27	50	9	24.3	-10.4	0.3	-65.6	0.6
Briggsdale	2022-07-27	75	10	23	-11.5	0.2	-67.6	0.7
Briggsdale	2022-08-01	50	12	23.4	-10.7	0.2	-67	0.7
Briggsdale	2022-08-01	75	13	22.4	-12.0	0.2	-69.1	0.7
Briggsdale	2022-08-06	50	15	24	-10.5	0.2	-65	0.6
Briggsdale	2022-08-06	75	16	22.9	-12.1	0.2	-68.8	0.7
Seibert	2022-06-19	25	2	24.2	-8.3	0.2	-59.8	0.6
Seibert	2022-06-19	50	3	22	-7.8	0.2	-57.8	0.6
Seibert	2022-06-19	75	4	19.4	7.4	0.2	-7.6	0.7
Seibert	2022-06-24	25	5	24	-8.7	0.2	-58.7	0.7
Seibert	2022-06-24	50	6	22.2	-7.9	0.2	-56.7	0.7
Seibert	2022-06-24	75	7	20.5	4.9	0.2	15.1	0.6
Seibert	2022-06-29	25	8	23.2	-7.4	0.2	-56.9	0.6
Seibert	2022-06-29	50	9	21.8	-9.1	0.2	-56.7	0.7
Seibert	2022-06-29	75	10	21	-5.6	0.2	-42.1	0.6
Seibert	2022-07-04	25	11	25	-8.7	0.2	-60.6	0.7
Seibert	2022-07-04	50	12	23.3	-9.9	0.2	-58.8	0.6
Seibert	2022-07-04	75	13	21.5	-8.5	0.2	-55.7	0.7
Oglala Ntl. Grassland	2022-06-25	25	2	23.0	-11.8	0.2	-101	0.7
Oglala Ntl. Grassland	2022-06-25	50	3	22.8	-16.7	0.2	-119.3	0.7
Oglala Ntl. Grassland	2022-06-25	75	4	21.5	-15.3	0.2	-115.5	0.8
Oglala Ntl. Grassland	2022-06-29	25	5	25.0	-14	0.2	-106.2	0.7
Oglala Ntl. Grassland	2022-06-29	50	6	22.8	-16.7	0.2	-120.6	0.7
Oglala Ntl. Grassland	2022-06-29	75	7	21.3	-15.8	0.2	-115.2	0.7
Oglala Ntl. Grassland	2022-07-04	25	8	25.0	-14	0.2	-102.2	0.7
Oglala Ntl. Grassland	2022-07-04	50	9	23.0	-16.8	0.2	-118.3	0.6
Oglala Ntl. Grassland	2022-07-04	75	10	22.0	-15.5	0.2	-114.7	0.6
Oglala Ntl. Grassland	2022-07-09	25	11	23.0	-14.1	0.2	-102.6	0.6
Oglala Ntl. Grassland	2022-07-09	50	12	22.8	-15.7	0.2	-116.4	0.7
Oglala Ntl. Grassland	2022-07-09	75	13	22.0	-15.7	0.2	-113.2	0.6
Oglala Ntl. Grassland	2022-07-14	25	14	23.0	-13.1	0.2	-99	0.6
Oglala Ntl. Grassland	2022-07-14	50	15	22.8	-14.9	0.3	-112.8	0.7
Oglala Ntl. Grassland	2022-07-14	75	16	22.0	-15.3	0.2	-111.2	0.7

905

906   Table 3. Results from the three field deployments of SWISS.
907

6. Discussion

6.1 QA/QC and field suitability tests

6.1.1 Dry Air tests

In Colorado, where these tests were completed, the ambient atmosphere during the summertime typically sits at a water vapor mole fraction between 10,000 - 20,000 ppm, and in winter the water vapor mole fraction can drop as low as 4000 ppm. If the flasks had been slowly equilibrating with the atmosphere, the flasks would have drifted to much higher water vapor molar fractions. If the flasks did not drift towards higher water vapor mole fractions, we felt confident that the flasks are resistant to atmospheric intrusion after they have been flushed with dry air. We chose a timescale of seven days for the dry air tests because we found that in a low-humidity environment, seven days was enough time to meaningfully observe leaks, while being ~~a~~ short enough ~~timescale~~ to ~~be able to continue to~~ work through the QA/QC process efficiently. For example, ~~in supplemental figure 4, we show the~~ results of two sequential dry air tests on the SWISS unit Toblerone (~~supp~~supplemental~~lemental~~ F~~f~~ig~~.ure~~ 24). ~~We, ~~show that it is possible to drastically reduce leaks that allow ambient water vapor in the air from intruding into the flasks by tightening and/or replacing problematic fittings (both those attached to the glass flasks and those on the Valco valve) and in some cases the glass flask itself. D~~F~~uring~~or~~ the final seven~~-~~day dry air tests, ~~the ~~most flasks ~~were able to ~~maintained a water vapor mole fraction ~~typically ~~less than 400 ppm, and all flasks maintained a water vapor mole fraction of less than 700 ppm (Fig. 34). ~~In Colorado, the ambient atmosphere during the summertime typically sits at a water vapor mole fraction between 10,000 - 20,000 ppm, and in winter the water vapor mole fraction can drop as low as 4000 ppm.~~the

Across all of the SWISS units, there is a bias towards a higher water vapor mole fraction for the first flask that is measured (port one on every valve is the flask bypass loop, so the first flask is flask two), which suggests a methodological source of higher water vapor concentration rather than ~~an issue with ~~Swagelok fitting tightness problems. There are two potential sources ~~of ~~for this issue. First, it is possible that not all of the atmospheric water vapor was flushed from the line that connects to the CRDS prior to the start of the measurements, but by the time the second flask is measured, the lines between the SWISS and CRDS have been sufficiently flushed, ~~and so there is~~creating bias in the first flask measured. ~~But, by the second flask, the lines between the SWISS and CRDS have been sufficiently flushed.~~ This hypothesis could be tested by ~~taking care to ~~flushing~~flush~~ all of the gas lines with dry air ~~until the water vapor mixing ratio is below 200 ppm~~to progressively lower water vapor mixing ratios prior to measuring any flasks, to see what minimum ratio is required to eliminate this bias. Lab protocols can then be adjusted to flush all gas lines to this level. Similarly, it is possible that during the filling phase, not all of the atmospheric vapor has been flushed out of the Drierite system before starting the fill process. This hypothesis is supported by the systematic decrease in water vapor mole fraction across flasks in the Toblerone unit (Fig. 3, right panel). As a result of these biases, we now flush the Drierite for at minimum 30 minutes prior to the start of the experiment.

~~This shows we can reduce the leakiness of the flasks.~~In addition to testing the ~~overall ~~leakiness, ~~T~~the dry air test ~~is ~~also provided ~~an easy~~useful baseline ~~test that~~from which ~~allowed us ~~to test building materials. For example, in supplemental figure 5, we show the results of sequential seven day and 27-day dry air tests where we replaced stainless steel tubing and fittings

Commented [KS1]: this seems useful to put earlier in the paragraph, as an expectation statement of what we are trying to prevent happening.

Commented [REH2R1]: Help

with PTFE Swagelok fittings with 1/8 inch PTFE tubing. We thought that PTFE fittings would be advantageous because they are much easier to install and are significantly lighter, and would therefore be helpful when there are weight constraints. However, ~~B~~based on the very limited testing we did, PTFE fittings and tubing *may be* sufficient to store water for up to a single week, but on longer timescales (e.g. 27 days) we observed greater exchange and leaking than with the stainless steel fittings. We encourage any future user using this modification to rigorously test these fittings on a timescale appropriate for their application.

~~We found that in a low-humidity environment, we needed a week to really see leaks, but this timescale would likely be shorter in more humid locations. If the flasks allowed in a significant amount of atmosphere, the flasks would have had much higher water vapor molar fractions. This suggests that the system is resistant to atmospheric intrusion.~~

~~There seems to be a systemic bias towards a high water vapor mole fraction for the first flask that is measured (flask 2). There are two potential analytical sources of this. First, its possible that during the filling phase, not all of the atmospheric vapor has been flushed out of the system before starting the fill process. Similarly, it is possible that not all of the atmospheric water vapor was flushed from the line that connects to the CRDS prior to the start of the measurements.~~

6.1.2 Water vapor tests

Our initial goal with the water vapor tests was to ~~show that~~test whether the measured water vapor isotope values at the end of the two-week holding period were normally distributed about 0 within the uncertainty limits of the water vapor probes (Oerter et al., 2016). This was a reasonable goal given the similarities in probe set-up and the plumbing design between the SWISS and the IsoWagon system. But, the most salient result of the water vapor tests is that there is a consistent positive offset between the input isotope values and the isotope values measured at the end of the two-week experiments (Figs 4B, 5B). The positive offset in both $\delta^{18}O$ and δ^2H values is consistent across 11 different tests, using six different SWISS and three different input water isotope values.

~~The in-lab water vapor tests served three functions: 1) they allowed us to test the best method for measuring soil water vapor at fairly high water vapor mole fractions that might be representative of field conditions (i.e. > 25,000 ppm), 2) to test if there is any systemic bias introduced through the building materials or measurement schema, and, 3) test whether soil water vapor samples can yield reliable stable isotope values.~~

~~We completed 11 water vapor tests using 6 SWISS units and three analytical sessions, resulting in 164 measurements of water vapor. Across the three analytical sessions, three waters with different isotopic compositions were used to produce water vapor (1 heavy, 1 intermediate, and 1 light).~~ If there was alteration of original values due to leaky flasks, we might expect the $\delta^{18}O$ and δ^2H values to converge on the $\delta^{18}O$ and δ^2H value of the atmosphere. For example, we might expect water vapor from the light water test to have the most significant change in isotope value, towards that of the ambient atmosphere. Instead, the ~~Figures 4 and 5 demonstrate that there is a consistent offset in both $\delta^{18}O$ and δ^2H of the water vapor from the start of storage to the end for all three analytical sessions. After removing outliers from the dataset, there remains a consistent bias across all SWISS boxes and analytical sessions (Figs 5B, 6B). The~~ consistency across >135 flasks, different starting water vapor isotope values, sample introduction methods, and multiple analytical sessions suggests that this difference is a function of the storage and measurement process. ~~Additionally~~In particular, the normality of the

998 distribution ~~suggests~~ whatever the origin of the offset is, ~~that~~ there is a systematic bias that we
999 can reliably correct for.
1000
1001 *6.1.2.1 Offset correction*
1002 To correct our data ~~create an~~for this offset ~~correction, w~~We chose to use the median value
1003 as an offset correction ~~over~~rather than the mean of the normal distribution, because the median is
1004 not biased by major outlier isotope values that reflect abnormal values that go beyond analytical
1005 noise, such as a slow but major leak that changes the values far beyond the basic offset seen in
1006 the dataset. The calculated average offset is 1.0‰ and 2.6‰ for $\delta^{18}O$ and $\delta^{2}H$, respectively.
1007 After applying these values as an offset correction to the data, ~~the~~ most flasks also fall within the
1008 uncertainty of the water vapor permeable probes ($\delta^{18}O = \pm0.5‰$ and $\delta^{2}H = \pm2.4‰$, Oerter et al.,
1009 2016), and the values are distributed about 0 (Figs. 4C, 5C).
1010 However, the uncertainty of the SWISS system ~~overall~~ is higher than that of the probes
1011 alone. Based on the results of the water vapor tests, we estimate the uncertainty of the SWISS at
1012 $\pm0.9‰$ and $\pm3.7‰$ for $\delta^{18}O$ and $\delta^{2}H$, respectively using the interquartile range (IQR) of the
1013 water vapor test results after removing outliers from the dataset. We prefer the IQR over the
1014 calculated standard deviation of the normal distribution, because IQR is not biased by outlier
1015 values. This level of uncertainty is large relative to other methods, but is sufficient for many
1016 critical zone applications, given the magnitude of seasonal variability in the top ~50 cm of a soil
1017 profile that can be observed in natural systems (e.g. Oerter et al., 2017; Quade et al., 2019). We
1018 also expect that uncertainties will decrease~~In the future, this uncertainty estimate can be~~
1019 ~~improved both by~~ with ~~further~~future lab-based or near research facility testing and by comparing
1020 the SWISS against other soil water extraction methods.
1021 The relationship between $\delta^{2}H$ values and $\delta^{18}O$ values in a dual-isotope plot ~~gives us~~
1022 ~~some~~provides insight into the mechanism driving the offset ~~correction~~. Without an offset
1023 correction applied, the slope of the relationship between $\delta^{2}H$ and $\delta^{18}O$ is 3.14 ($R^{2} = 0.62$)
1024 (Supplemental Fig. 4). This slope is only slightly higher than evaporation under pure diffusion
1025 (Gonfiantini et al., 2018). This suggests that the offset ~~correction~~ is likely driven by diffusion and
1026 will likely vary according to climate of the lab. For example, in a dry climate like Colorado, the
1027 water vapor concentration in the flask is significantly higher than the atmosphere, creating a
1028 larger diffusive gradient potential than for a lab in a more humid climate. We therefore~~,~~ strongly
1029 encourage future users to test their SWISS under climate conditions ~~appropriate~~similar for their
1030 applications. Further, we encourage users who might use the SWISS as part of a tracer study that
1031 uses labeled heavy water to test the SWISS with labeled waters prior to their field experiments to
1032 verify reliability.
1033
1034 ~~*In figures 5C and 6C, we show the results of 3 water vapor tests from the August 2022 analytical*~~
1035 ~~*session, with an offset correction applied. 43 of the 45 measured flasks faithfully retained the*~~
1036 ~~*starting δ18O value of the water vapor, and 37 of the 45 measured flasks faithfully retained the*~~
1037 ~~*starting δ2H value of the water vapor. Additionally, after the offset correction was applied, most*~~
1038 ~~*flasks also fall within the uncertainty of the water vapor permeable probes (δ18O = 0.5‰ and*~~
1039 ~~*δ2H =*~~6.1.2.2 Comparing sample introduction methods~~*2.4‰).*~~
1040 Supplemental figure 6 shows a kernel density estimate plot of the results from two water
1041 vapor test sessions, with the offset correction applied. During the March 2022 session, flasks
1042 were measured using the dead-end pull sample introduction method and during the August 2022
1043 session, flasks were measured using the dry air carrier gas sample introduction method. There is

1044 no significant difference in the measured difference between the two sample introduction
1045 methods. ~~W~~That said, we prefer the dry air carrier gas method, because it is far simpler to control
1046 the water vapor mixing ratio, and optimize the concentration to be around 25,000 ppm, which is
1047 the concentration at which the Picarro L2130-*i* is most reliable. The dry air carrier gas method
1048 also makes it ~~far~~ easier to control for and monitor for condensation in the stainless-steel tubing
1049 and vapor impermeable tubing, which can bias a measurement.
1050
1051

Site	Date	Sample Depth (cm)	Flask	T	δ¹⁸O (‰)	δ¹⁸O (‰) Analytical Error	δ²H (‰)	δ²H (‰) Analytical Error
Briggsdale	7/17/22	50	3	23	-10.6	0.2	-63.4	0.6
Briggsdale	7/17/22	75	4	23	-12.1	0.2	-69	0.7
Briggsdale	7/22/22	50	6	23	-10.5	0.3	-64	0.7
Briggsdale	7/22/22	75	7	23	-11.8	0.2	-68.3	0.6
Briggsdale	7/27/22	50	9	23	-10.3	0.3	-64.3	0.6
Briggsdale	7/27/22	75	10	23	-11.5	0.2	-67.6	0.7
Briggsdale	8/1/22	50	12	23	-10.7	0.2	-66.6	0.7
Briggsdale	8/1/22	75	13	23	-12	0.2	-69.7	0.7
Briggsdale	8/6/22	50	15	23	-10.4	0.2	-63.9	0.6
Briggsdale	8/6/22	75	16	23	-12.1	0.2	-68.9	0.7
Seibert	6/19/22	25	2	23	-8.2	0.2	-58.6	0.6
Seibert	6/19/22	50	3	23	-7.9	0.2	-58.8	0.6
Seibert	6/24/22	25	5	23	-8.6	0.2	-57.6	0.7
Seibert	6/24/22	50	6	23	-8	0.2	-57.5	0.7
Seibert	6/29/22	25	8	23	-7.4	0.2	-56.7	0.6
Seibert	6/29/22	50	9	23	-9.2	0.2	-58	0.7
Seibert	7/4/22	25	11	23	-8.6	0.2	-58.6	0.7
Seibert	7/4/22	50	12	23	-9.9	0.2	-58.5	0.6
Oglala Ntl. Grassland	6/25/22	25	2	23	-11.8	0.2	-101.0	0.7
Oglala Ntl. Grassland	6/25/22	50	3	22.8	-16.7	0.2	-119.3	0.7
Oglala Ntl. Grassland	6/25/22	75	4	21.5	-15.3	0.2	-115.5	0.8
Oglala Ntl. Grassland	6/29/22	25	5	25	-14.0	0.2	-106.2	0.7
Oglala Ntl. Grassland	6/29/22	50	6	22.8	-16.7	0.2	-120.6	0.7

Oglala Ntl. Grassland	6/29/22	75	7	21.3	-15.8	0.2	-115.2	0.7
Oglala Ntl. Grassland	7/4/22	25	8	25	-14.0	0.2	-102.2	0.7
Oglala Ntl. Grassland	7/4/22	50	9	23	-16.8	0.2	-118.3	0.6
Oglala Ntl. Grassland	7/4/22	75	10	22	-15.5	0.2	-114.7	0.6
Oglala Ntl. Grassland	7/9/22	25	11	23	-14.1	0.2	-102.6	0.6
Oglala Ntl. Grassland	7/9/22	50	12	22.8	-15.7	0.2	-116.4	0.7
Oglala Ntl. Grassland	7/9/22	75	13	22	-15.7	0.2	-113.2	0.6
Oglala Ntl. Grassland	7/14/22	25	14	23	-13.1	0.2	-99.0	0.6
Oglala Ntl. Grassland	7/14/22	50	15	22.8	-14.9	0.3	-112.8	0.7
Oglala Ntl. Grassland	7/14/22	75	16	22	-15.3	0.2	-111.2	0.7

Table 3. Results from the three field deployments of SWISS.

suggests that there is a systematic bias that we can reliably correct for. We chose to use the median value as an offset correction over the mean of the normal distribution, because the median is not biased by higher isotope difference values that are a complex combination of systematic bias and slow leaking. The calculated average offset is 1.0‰ and 2.6‰ for $\delta^{18}O$ and $\delta^{2}H$, respectively.

Based on the results of the water vapor tests, we estimate the uncertainty of the SWISS at 0.9‰ and 3.7‰ for $\delta^{18}O$ and $\delta^{2}H$, respectively using the interquartile range (IQR) of the water vapor test results after removing outliers from the dataset. We prefer the IQR over the calculated standard deviation of the normal distribution, because IQR is not biased by outlier values. In figures 5C and 6C, we show the results of 3 water vapor tests from the August 2022 analytical session, with an offset correction applied. 43 of the 45 measured flasks faithfully retained the starting $\delta^{18}O$ value of the water vapor, and 37 of the 45 measured flasks faithfully retained the starting $\delta^{2}H$ value of the water vapor. Additionally, after the offset correction was applied, most flasks also fall within the uncertainty of the water vapor permeable probes ($\delta^{18}O = 0.5$‰ and $\delta^{2}H = 2.4$‰).

Supplemental figure 3 shows a kernel density estimate plot of the results from two water vapor test sessions, with the offset correction applied. During the March 2022 session, flasks were measured using the dead-end pull sample introduction method and during the August 2022 session, flasks were measured using the dry air carrier gas sample introduction method. There is no significant difference in the measured difference between the two sample introduction methods. We prefer the dry air carrier gas method, because it is far simpler to control the water vapor mixing ratio, and optimize the concentration to be around 25,000 ppm, which is the concentration at which the Picarro L2130-i is most reliable. The dry air carrier gas method also makes it far easier to control for and monitor for condensation in the stainless steel tubing and vapor impermeable tubing, which can bias a measurement.

6.1.3 Field suitability tests

The long dry air tests in the field are a useful complement to the shorter in-lab tests because they test the reliability of the system at field-deployment timescales. It is clear from the 34 and 43 day tests that the flasks are reasonably resistant to leaks on the timescale of a normal 4 – 6 week deployment to be able maintain the composition of vapor in the flasks (Fig. 6A). These tests also give us confidence that flasks filled later in the sampling sequence do not take on an atmospheric signal prior to sampling. There are a few possibilities to explain the poorer performance of the Toblerone SWISS unit during the 52-day test. (Fig. 6A). The first is that there is a real threshold past which the SWISS are no longer able to retain samples. However, this explanation would suggest that there should be a gradual decrease in performance across the three tests, which we do not observe. The alternative explanation is that the poor performance is a result of inter-unit variability. The 52-day test was the first long-term test and was performed in August 2021. In August 2021, we were continuing to build new SWISS units and continuing to learn from each successive round of QA/QC, so it seems plausible that there were unidentified problems with the SWISS unit Toblerone that were solved before the water vapor tests in August 2022.

In Figure 7A, we observe that the flasks typically maintained a low water vapor mole fraction (< 1000 ppm) under field conditions, and at timescales relevant to 4-6 week field deployments (34 - 43 days). The 34 day test was done during June 2022, and therefore tests the SWISS under warm

summertime conditions. The 43 day test was done in October 2021, which included nights where temperatures fell below 0°C, and therefore tests the suitability of the SWISS to maintain integrity under freezing conditions. We observe that the SWISS did considerably worse at maintaining a low water vapor mole fraction over a 52 day time period during similar summertime conditions as compared to the 34 - 43 day time period. Over the 52 days, seven flasks maintained a water vapor mole fraction less than 1000 ppm and the remaining 8 had a water vapor mole fraction between 1000 - 2500 ppm. Though the SWISS performed considerably worse after 52 days than it did from 34 - 43 days, it is important to note that the atmospheric water vapor mole fraction during the storage time period was likely 15,000 - 20,000 ppm, and so the measured values demonstrate that the SWISS are still quite resistant to atmospheric intrusion at that timescale.

In figure 6~~7~~B, the data show that the flasks ~~faithfully~~ preserved the $\delta^{18}O$ value of both flash-evaporated and atmospheric water vapor ~~produced using the vapor permeable probe and the atmosphere~~ over a seven- day period. One flask was removed from the dataset (flask eight), because there was ~~noticeable~~ visible condensation in the clear impermeable tubing during the measurement phase, with an increase of > 5‰ for $\delta^{18}O$ during the measurement period. The condensation appeared as small (<1 mm) bubbles of water all along the impermeable tubing, but the bubbles were concentrated near the connection between the SWISS and the impermeable tubing. Notably, the two flasks whose $\delta^{18}O$ ~~oxygen isotope~~ values do not overlap within uncertainty are more negative than expected, rather than drifting towards atmospheric values or values expected ~~with~~from ~~kinetic~~ diffusive fractionation. ~~It is possible that those samples were also affected by condensation at the start of the experiment; during condensation, we expect that ^{18}O will preferentially go into the liquid phase, and that the water vapor that enters the flask will have a lower than expected $\delta^{18}O$ value.~~

In contrast to the ~~oxygen isotope~~$\delta^{18}O$ value ~~results,~~ ~~Surprisingly~~o, only 3 flasks filled with ~~either~~ flash evaporated ~~DI or light~~ water vapor overlap within uncertainty of the known δ^2H values, while four of the five flasks overlap within uncertainty of the estimated atmosphere isotope value. The flasks tend to drift towards the value of the atmosphere, but retain the overall data pattern from the oxygen isotope values.

The relatively high failure rate of th~~e~~is 'mock' field test was somewhat surprising given the results of the water vapor tests done in the laboratory. Going into the test, we suspected that flasks six and eight were slightly leaky based on previous water vapor tests; these were flasks that previously performed poorly, but did not 'fail' during the water vapor test. Once we collected the data, we compared~~evaluated~~ the data for flasks six and eight ~~relative~~ to other flasks in the sequence. During the measurement of flask eight, we observed condensation in the sample introduction lines, and because the isotope values were so different relative to other flasks, we felt confident in our exclusion of flask eight Flask six~~,~~ had ~~oxygen~~ $\delta^{18}O$ and ~~hydrogen isotope~~ δ^2H values similar to others from the same sampling source, and seemed to fall within the pattern as expected. Therefore, we chose to keep this data point in the dataset.

We hypothesize that one major problem with the mock field test dataset wa~~i~~s the creation of condensation in the sampling lines, as others have experienced in their setups (e.g. Quade et al., 2019; Kühnhammer et al., 2019). Of particular interest are the flasks that ha~~ve~~d a lower than expected ~~oxygen isotope~~ $\delta^{18}O$ value (flasks four and nine). It is possible that those samples were also affected by condensation, but in contrast to flask eight, which was excluded because of condensation during measurement, we think that these samples may have been altered because of condensation at the sampling stage.~~;~~ ~~D~~during condensation, we expect that ^{18}O will preferentially enter the liquid phase, and that the water vapor that enters the

1146 flask will have a lower than expected $\delta^{18}O$ value. The unique advantage of the SWISS is that it
1147 can operate independently, but with that comes the trade-off that ~~it may~~we cannot currently ~~be~~
1148 ~~possible to identify~~observe condensation in the lines ~~as it is happening~~during sample collection.
1149 To prevent condensation from forming, other users have warmed the impermeable tubing
1150 between the probes and the Picarro. The 'mock' field test data suggest that in many situations it
1151 may be worthwhile to warm the transfer tubing, but this should be done in a way that does not
1152 alter the thermal structure of the soil, and in remote settings, can operate safely independently.
1153
1154 **6.1.4 Lessons learned and recommendations from the QA/QC and field suitability tests:**
1155
1156 Our QA/QC process was a relatively efficient way to test the soundness of the SWISS
1157 units. Through the QA/QC process we were able to identify problems with units, and
1158 appropriately address them before deploying units to the field. We strongly recommend that any
1159 user deploying SWISS to the field to undertake the same, or similar, QA/QC process.
1160 The dry air test is a time-efficient and low-cost method for identifying flasks that are
1161 leaky and will not preserve the sampled water vapor isotope value~~s~~. It is useful during the
1162 building stage to identify fittings that need to be tightened or flasks that need to be replaced, and
1163 therefore we recommend these tests as a required ~~step prior to field~~ pre-deployment step for~~of~~
1164 future SWISS units. We found that it was most time and energy efficient to move onto the next
1165 level of QA/QC once 13 out of 15 flasks of a SWISS unit had passed the dry-air test, because
1166 frequently the remaining two flasks still had relatively low water vapor mole fractions (i.e. 500 –
1167 700 ppm), and we could sufficiently tighten the fittings prior to the start of the water vapor tests
1168 for them to be successful. The dry air test is a low time and expense burden that ~~it~~ can also be
1169 used to monitor SWISS units for normal wear-and-tear (e.g. a flask that cracked during transport)
1170 during deployment periods. Therefore, to ensure that SWISS units continue to operate as
1171 expected, we also recommend that dry air tests be done between field deployments on every
1172 SWISS unit. Lastly, we note that ~~,t therefore we recommend these tests as a required step prior to~~
1173 ~~field deployment of future SWISS units. For example, supplemental figure 4 shows that it is~~
1174 ~~possible to drastically reduce the water vapor mole fraction in a flask filled with dry air between~~
1175 ~~tests by tightening and/or replacing problematic fittings (both those attached to the glass flasks~~
1176 ~~and those on the valco valve) and in some cases the glass flask itself. This shows we can reduce~~
1177 ~~the leakiness of the flasks. The dry air test is also an easy baseline test that also allowed us to test~~
1178 ~~building materials. For example, in supplemental figure 5, we tested using PTFE swagelok~~
1179 ~~fittings with ⅛" PTFE tubing rather than stainless steel. These materials would be advantageous~~
1180 ~~because they are much easier to install and are significantly lighter. We found that these fittings~~
1181 ~~and tubing~~ *may be* ~~sufficient to store water for up to a single week, but on longer timescales (e.g.~~
1182 ~~27 days) we observed greater exchange and leaking than the stainless steel. We encourage any~~
1183 ~~future user using this modification to rigorously test these fittings on a timescale appropriate for~~
1184 ~~their application.~~ he dry air test could be modified based on available equipment (for example, if
1185 an instrument is available to measure trace atmospheric gases, that could be used instead).
1186 Based on the results of the long, field dry air test, we recommend that the water vapor
1187 storage time doesn't exceed 40 days for reliable results, or that the user undertake multiple dry
1188 air tests with either lower concentration benchmarks or longer duration if deployments may
1189 exceed 40 days.
1190

1191 From the water vapor tests, we get a sense of the accuracy and precision of the SWISS.
1192 The calculated uncertainty of the flasks (0.9‰ and 3.7‰ for $\delta^{18}O$ and δ^2H, respectively) is
1193 somewhat larger than the uncertainty associated just with the use of the water vapor probes
1194 (0.5‰ and 2.4 ‰ for $\delta^{18}O$ and δ^2H, respectively, Oerter et al., 2016), but is sufficient for many
1195 critical zone applications, given the magnitude of seasonal variability that can be observed in
1196 natural systems (e.g. Oerter et al., 2017; Quade et al., 2019).
1197 We opted to use a large flask volume because it allows us to measure a sample for long
1198 enough on a CRDS that we get reliable data, without interacting with vapor bound to the flask
1199 walls. The drawback of this, however, is that we must sample soil water vapor for a relatively
1200 long period of time (45 minutes). In supplemental figure 6, we show that the sampling regime,
1201 and particularly the length of time we pump dry air through the tubing, does not significantly
1202 alter the soil moisture content of the soil. Additionally, we demonstrate that the sampling regime
1203 we use does not introduce significant memory effects.
1204 Based on the results of the long, field dry air test, we recommend that the water vapor
1205 storage time doesn't exceed 40 days for reliable results, or that the user undertake multiple dry
1206 air tests with lower concentration benchmarks if deployments may exceed 40 days.
1207 Overall, the quality control and quality assurance as well as the field suitability tests the
1208 field suitability tests demonstrate that the SWISS units are able to faithfullycan retain the isotope
1209 values of water vapor collected using water vapor permeable probes. Like many other systems
1210 that measure dual isotopes, each system (i.e. $\delta^{18}O$ and δ^2H) must be evaluated separately. In
1211 general, we interpret oxygen isotope data with a higher degree of confidence than the hydrogen
1212 isotope data. As the automation test revealed however, even when the absolute δ^2H value is not
1213 correct, the general pattern can reveal information about soil water dynamics.
1214 Finally, Wwe opted to use a large flask volume because it allows us to measure a sample
1215 for long enough on a CRDS that we get reliable data, without interacting with vapor bound to the
1216 flask walls. The drawback of this, however, is that we must sample soil water vapor for a
1217 relatively long period of time (45 minutes). In supplemental figure 7, we show that the sampling
1218 regime, and particularly the length of time we pump dry air through the tubing, does not
1219 significantly alter the soil moisture content of the soil. Additionally, we demonstrate that the
1220 sampling regime we use does not introduce significant memory effects.
1221 One particular challenge with the vapor permeable probes, that others have noted, is
1222 condensation in any portion of the system (e.g. Quade et al., 2019; Kühnhammer et al., 2019) .
1223 As much as possible, it is helpful to have the impermeable tubing at warmer temperatures than
1224 the soil or water it is sampling. In many situations it may be worthwhile to warm the transfer
1225 tubing, but this should be done in a way that does not alter the thermal structure of the soil, and
1226 in remote settings, can operate safely independently. Additionally, taking care to ensure that the
1227 SWISS is evenly and lightly warmed in the lab setting helps to prevent condensation from
1228 forming in the stainless steel tubing and Valco valve.
1229
1230 **6.2 Field Deployments**
1231 In Figure 7 we show the results of three field deployments completed during summer
1232 2022 (Ttable 3). At the Oglala National Grassland site, we used the SWISS unit named Lindt to
1233 collect samples. During the August 2022 water vapor test on Lindt, all ofall the oxygen isotope
1234 $\delta^{18}O$ values fall within uncertainty of the system, and nine of the fifteen flasks hydrogen isotope
1235 δ^2H values fall within uncertainty of the system. Therefore, we interpret the $\delta^{18}O$ values with a
1236 highergreater amount of confidence and the δ^2H values with a lower amount of confidence (Figs.

A Oglala Nt'l. Grassland

Sample Date
● 2022–06–25
● 2022–06–29
● 2022–07–04
● 2022–07–09
○ 2022–07–14

Sample Depth (cm)
□ 25
◇ 50
△ 75
— — GMWL

B

Sample Depth (cm)
■ 25
◆ 50
▲ 75
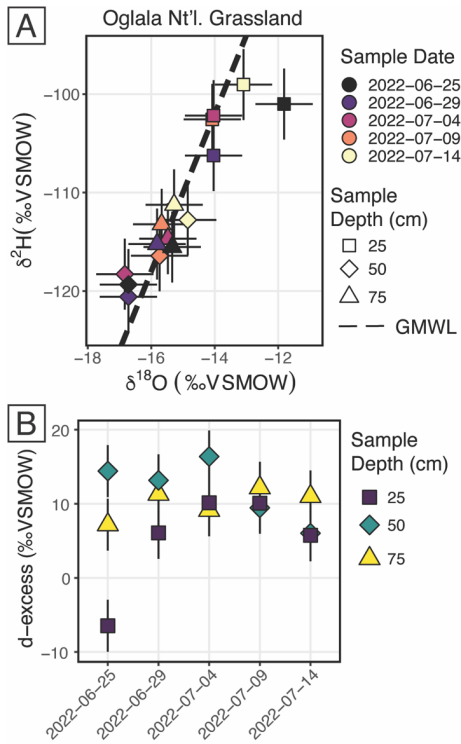
4C and 5C). We note that ~~most of~~ the $\delta^{18}O$ and δ^2H values broadly follow the same trends, and fall on the global meteoric water line (Figs. 7 and 8A). In general, soil water from 25 cm had higher $\delta^{18}O$ and δ^2H values than soil water from both 50 and 75 cm (Fig. 8A). Given that 4 of the 5 samples from 25 cm overlap with the GMWL and have a d-excess that overlaps with~~in error of~~ 10 ± 2.6‰, the soil water from that depth may reflect summer precipitation with higher $\delta^{18}O$ and δ^2H values. Soil water from 75 cm had intermediate $\delta^{18}O$ and δ^2H values for most of the study period, and soil water from 50 cm depth had the lowest $\delta^{18}O$ and δ^2H values for most of the study period, which may reflect a more mean-annual or winter precipitation biased value. ~~The d-excess value of soil water collected from 75 cm is centered around a global meteoric water line value of 10‰ (Fig. 8B).~~ Based on data available from the National Weather Service (Chadron, NE), there were likely significant precipitation events on 2022-06-25 and 2022-07-08 at the field site. There is a significant shift to lower $\delta^{18}O$ values at a sampling depth of 25 cm between 2022-06-25 and 2022-06-29, as well as a marked increase in the d-excess value (Fig. 8A). We interpret this shift as infiltration of precipitation with lower $\delta^{18}O$ values, ~~and~~which is supported by a return of d-excess values to ~10‰ (Fig. 8A). The National Weather Service reported 21.33 mm (0.84 inches) ~~0.84 inches~~ of rain at Chadron Municipal Airport, approximately 50 km from the study site on 2022-07-08, which likely was associated with at least some precipitation at our field site. Following the significant rain event on 2022-07-08, we observe a marked increase in the stable isotope value of water vapor from a sampling depth of 50 cm, towards values that are much closer to those at 25 cm depth. These data suggests that soil water isotopes at 50 cm in this silt-loam Aridisol may be fairly sensitive to large individual precipitation events, while at 75 cm soil water isotopes remain comparatively uniform. Future work should address how drought conditions, storm size, pore size distribution, and soil clay mineralogy influence the variability of soil water isotopes with depth. ~~This indicates that after a large precipitation event, there is mixing and the creation of a far more uniform soil water isotope profile to a depth of 50 cm, but at the depth of 75 cm, the oxygen isotope data remain fairly uniform across the sampling period.~~

1283
1284
1285
1286
1287
1288
1289
1290
1291
1292
1293
1294
1295
1296
1297 Figure 8. Results from the Oglala National Grassland, NE field site. A) δ²H vs. δ¹⁸O, where the dashed line is the global
1298 meteoric water line. The shape of the depth sampled matches figure 7, and the color of the points is the date on which the
1299 soil water was sampled B) A plot of d-excess. Note, both the color and shape match figure 7.
1300
1301
1302   At Briggsdale, CO we used the SWISS named Raclette to collect soil water vapor
1303 samples. Data from 25 cm depth at Briggsdale, CO were discarded because the water vapor mole
1304 fraction was much lower than would be expected given the soil temperature (i.e. < 15,000 ppm).
1305 The gravimetric water concentration at that soil depth at the time of sampling was approximately
1306 4% through the sampling period. Given the low water concentration, it is possible that there was
1307 simply not enough water vapor to sufficiently sample. Data from 25 cm depth at Briggsdale, CO
1308 were discarded because the water vapor mole fraction was much lower than would be expected
1309 given the soil temperature (i.e. < 15,000 ppm). The gravimetric water concentration (GWC) at
1310 that soil depth at the time of sampling was approximately 4% through the sampling period.
1311 Future work should include a multiple-method (e.g. cryogenic extraction, centrifugation, etc.)
1312 comparison of soil water isotopes at low water contents to better understand what these samples
1313 might represent, and if they are actually representative of soil conditions.
1314   Based on the results of the August 2022 water vapor test done on Raclette where all
1315 flasks fell within uncertainty of the SWISS system for both $\delta^{18}O$ and δ^2H, except for flask 11
1316 (Figs. 4C and 5C), which corresponds to the 25 cm depth sample from 2022-07-27, we interpret
1317 all of the data with a higher level of greater confidence. This sampleFlask 11 corresponds to the
1318 25 cm depth sample from 2022-07-27, and was already removedculledculled from the dataset
1319 because of low water vapor mole fraction associated with the very dry soil. The soil water $\delta^{18}O$
1320 and δ^2H values from a sampling depth of 50 cm and 75 cm overlap within uncertainty, but the
1321 soil water $\delta^{18}O$ and δ^2H values from 50 cm have a higher isotopic valueare higher than the
1322 samplesisotope values from 75 cm. All of the data from within each sampling depth group (i.e.
1323 50 cm and 75 cm) overlap within uncertainty, conforming to the expectation that soil water from
1324 these sampling depths should be fairly invariant (e.g. Oerter et al., 20197). There were
1325 precipitation events at the study site on 2022-07-24, 2022-07-28 and 2022-07-31. It is possible
1326 that the slight negative shift in both $\delta^{18}O$ and δ^2H on 2022-08-01 reflects infiltration of
1327 precipitation to those depths, but this is not certain given that all of the measurements from
1328 within a sampling depth overlap within uncertainty.

At Seibert, CO we used the SWISS named Toblerone to collect soil water vapor samples. The soil water isotope data from 75 cm depth at this site offer a few useful lessons for future users. The two~~first most basic~~key observations of the data from 75 cm depth are that ~~is~~that for ~~the first two samples, the~~ ~~isotope values are unreasonably high (i.e. have~~$\delta^{18}O$ and δ^2H values are much higher than the other two sampling depths d ~~oxygen isotope values)~~, and that the ~~hydrogen~~ δ^2H and ~~oxygen isotope~~ $\delta^{18}O$ values do not move in parallel with each other. While measuring these samples we observed condensation in the impermeable tubing at the point where the SWISS connects to the impermeable tubing. Additionally, when we heated the stainless steel tubing that connects the tubing flask and Valco valve we observed a rapid increase in water vapor mole fraction (1000's of ppm over <30 seconds) that was accompanied by a rise in stable isotope value. During these measurements, we were rarely able to get a stable isotope value measurement window, and instead the stable isotope value of the vapor increased continually through the measurement. It is for these reasons that we feel confident in discarding the stable isotope data from 2022-06-19 – 2022-06-29. The final measurement from 75 cm depth on 2022-07-04 approaches a reasonable isotope value when compared to isotope values from the other two depths, and that sample had ~~far~~ fewer condensation problems during measurement. However~~., but~~ because we have no sequential context for what a reasonable value for this depth is, we ~~have chosen to~~ discarded ~~discard~~ that value as well. For that final 75 cm sample, we were more successful because we warmed the entire length the vapor impermeable tubing, as well as the stainless-steel tubing, flask, and Valco valve evenly so that there were no temperature gradients across the vapor path. If the condensation had only been in the impermeable tubing it would have been much easier to ~~'rescue'~~successfully analyze these samples by just closing off the flask and running dry air through the tubing to remove condensation, but because condensation was also occurring in the stainless steel tubing between the flask and Valco valve, ~~it became much more challenging to 'rescue' samples~~this was not possible. It remains unclear why condensation was such a significant problem for samples from that depth as opposed to samples from different depths in the same SWISS. Future work should include further testing of the SWISS across different water contents and temperatures to better understand why the phenomenon may have occurred.

~~Data from 75 cm depth at Seibert, CO were discarded because of evidence of~~ ~~condensation during the measurement of the flasks associated with that sampling depth.~~ Based on the results of the August 2022 water vapor test done on Toblerone, we interpret all ~~of the~~ data from 50 cm and 25 cm depth with ~~a high degree of~~high confidence, except for Flask 3, which is the 50 cm sample from 2022-06-19 (Figs. 4C and 5C). Unlike data from the other two field sites, soil water from 25 cm and 50 cm overlap within uncertainty. There were two precipitation events at the field site during the sampling period on 2022-06-25 and 2022-07-01, but both events were quite small (<~~0.5~~0.02 ~~inches~~mm, CoAgMet). There is no significant influence of the precipitation events on the $\delta^{18}O$ and δ^2H values. The >1.0‰ increase in $\delta^{18}O$ values on 2022-06-29 is surprising given that there is not a comparable magnitude increase in δ^2H value, and that the values measured from 2022-07-04 more closely match the $\delta^{18}O$ and δ^2H values from the two earlier sampling days. There are two potential explanations for this data. First, that this shift is a real signal from an evaporation driven increase in the $\delta^{18}O$ value, and the ~~reset~~shift back to a ~~lighter~~lower $\delta^{18}O$ value on 2022-07-04 is due to the infiltration of precipitation. ~~A different way to see this is through the~~ This explanation is corroborated by a, which could also explain the ~~low~~ d-excess value associated with this measurement (Supplemental Fig. ~~SI~~ 8 9). The second possible explanation is that the 25 cm sample from 2022-06-29 is influenced by condensation at

1375 the time of sampling. Dew point at the field site on 2022-06-29 significantly decreased as
1376 compared to the other sampling days to a monthly minimum of 20.6°C (CoAgMet). It is possible
1377 that environmental conditions encouraged the formation of condensation in the impermeable
1378 tubing at the time of sampling. There were no obvious signs of condensation during the time of
1379 measurement in the lab. These results highlight the utility of having broad contextual
1380 environmental data to aid in the interpretation of soil water isotope data.
1381 All together, these three soil water isotope datasets demonstrate two main findings. First,
1382 data from these samples show that the differences between field sites isare easily resolvable
1383 using the SWISS. For example, at 50 cm depth the oxygen isotopes range between -14.4 to -
1384 16.3‰, -9.9 to -10.3‰, and -7.4 to -9.3‰ for the Oglala, Briggsdale and Seibert sites,
1385 respectively. These differences likely reflect differences in the stable isotope composition of
1386 precipitation and infiltration and evaporation dynamics. Second, the sample data retrieved from a
1387 SWISS are sufficiently precise to be able to meaningfully resolve vertical profile soil water
1388 isotope data. For example, at the Oglala National Grassland field site, soil water from 25 cm
1389 clearly has higher δ^{18}O and δ^2H values as compared to soil water from a depth of 50 and 75 cm.
1390
1391
1392 **6. 3 Future improvements and future work**
1393 One significant SWISS unit hardware improvement that could be made would be to
1394 install a heating implement to the flasks. One source of uncertainty on the current system is the
1395 potential effect of uneven heating of the flasks prior to measurement which may create
1396 temperature gradients that are large enough to allow for condensation when warm vapor meets a
1397 slightly colder spot. This could be improved in subsequent iterations of the SWISS with the
1398 addition of heat tape or blankets that can deliver controlled heat and create consistent amounts of
1399 heattemperatures. This improvement ewould also help limit the amount of manual intervention
1400 needed during measurement, and could improve automation of flask measurement. Additionally,
1401 finding a way to safely and automatically heat the impermeable tubing that connects the water
1402 vapor probes and the SWISS in a way that doesn't change the inherent thermal structure of the
1403 soil, and is safe for unmonitored use, would help to prevent the formation of condensation in the
1404 field and reducelimit the number of uncertaintiesy onrelated to measurementssampling.
1405 In addition,
1406 Wwe have made a few improvements to the automation system that were not
1407 implemented for the data presented in this contribution, but will be part of future deployments.
1408 First, we will track conditions inside the SWISS with a temperature and relative humidity sensor
1409 inside the case. Second, we plan to eliminate the power inverter by powering both the Valco
1410 valve and mass flow controller with VDC using a power step up controller. Lastly, we will add
1411 an IoT cellular router to be able to remotely monitor and control the SWISS units. This would be
1412 particularly helpful if there is a sampling day that is unexpectedly cold or when the dew point at
1413 the field site is unexpectedly low and we expect condensation to form more readily form in the
1414 field, or if there is a precipitation event that we are really interested in capturing, because with
1415 the IoT cellular router we could remotely alter the sampling plan.
1416 While the improvements and additional testing we have done to the SWISS in this
1417 contribution represent a significant step forward, additional work should be done to make the
1418 system more useable by the ecohydrology community. We have rigorously tested the SWISS in
1419 the lab, and demonstrated a few ways in which the SWISS can fail in field settings. A full
1420 comparison of how soil water isotope data collected using a SWISS as compared to other in situ

1421 (both vapor probes and lysimeter) and destructive sampling methods would shed light on the
1422 accuracy and precision of our system, and the applicability of our lab-based experiments to the
1423 field. These experiments should be carefully designed ~~to take~~with considerations of soil grain
1424 size, soil water content, expected isotope values, and climate. ~~Finally, there are two future~~
1425 ~~considerations for field deployments. The first is finding a way to safely and automatically heat~~
1426 ~~the impermeable tubing that connects the water vapor probes and the SWISS in a way that~~
1427 ~~doesn't change the inherent thermal structure of the soil, and is safe for unmonitored use.~~
1428 Additionally, we plan to test SWISS unit resilience during air travel so that these units can be
1429 used at field sites that are not within driving distance of a research facility.

Conclusions

1431   We presented the evolution of the soil water isotope storage system (SWISS) from a
1432 prototype to a fully built out and tested system. We also presented a quality control and quality
1433 assurance procedure that we strongly recommend future users undertake ~~can be used~~ to ensure
1434 the reliable storage of soil water vapor over long time periods (up to 40 days). In addition, these
1435 quality control and quality assurance tests shed light on the accuracy and precision of the
1436 SWISS. After applying an offset correction, we determine the ~~overall~~ precision of the SWISS to
1437 be $\pm$0.9‰ and ~~3~~$\pm$3.7‰ for δ^{18}O and δ^2H, respectively. In a field setting, flasks reliably resist
1438 atmospheric intrusion. Additionally, the proposed sampling schema does not introduce
1439 significant memory effects. Lastly, we demonstrate that the current precision of the SWISS still
1440 allows us to distinguish between field sites and between soil water dynamics within a single soil
1441 column. Taken as a whole, these data show that the SWISS can be used as a tool to answer many
1442 emerging ecohydrological questions, and will enhance researchers' ability to collect soil water
1443 isotope datasets from more remote and traditionally understudied field sites.

Acknowledgements

1445   We thank the numerous field assistants who helped to make the field work presented in
1446 this paper possible, including Spencer Burns, Anne Fetrow, Sarah Brookins, Juliana Olsen-
1447 Valdez, and Haley Brumberger. We acknowledge that both field work and laboratory work for
1448 this study w~~as~~ere done on the traditional territories and ancestral homelands of the Arapahoe,
1449 Ute and Cheyenne peoples. This work was supported by startup funding from CU Boulder and
1450 NSF funding from grant EAR-2023385 awarded to K. Snell. Additionally, this work was
1451 supported by the University of Colorado Boulder Beverly Sears Research Grant and the Clay
1452 Minerals Society Graduate Student Research Grant both awarded to R. Havranek. CUBES–SIL
1453 is a CU Boulder Core Facility associated with RRID: SCR_019300.

1454

Author contribution

Rachel E. Havranek: ~~original draft, c~~conceptualization, methodology, investigation, formal analysis, funding acquisition, writing – wrote original draft, review and editing. Kathryn E. Snell: c~~C~~onceptualization, m~~M~~ethodology, w~~W~~riting – review & editing, funding acquisition. Sebastian H. Kopf: c~~C~~onceptualization, m~~M~~ethodology, w~~W~~riting – review & editing. Brett Davidheiser-Kroll: c~~C~~onceptualization, c~~M~~ethodology, w~~W~~riting – review & editing. Valerie Morris: m~~M~~ethodology, w~~W~~riting – review & editing. Bruce Vaugh: m~~M~~ethodology, w~~W~~riting – review & editing.

Competing interests

The authors declare no competing interests.
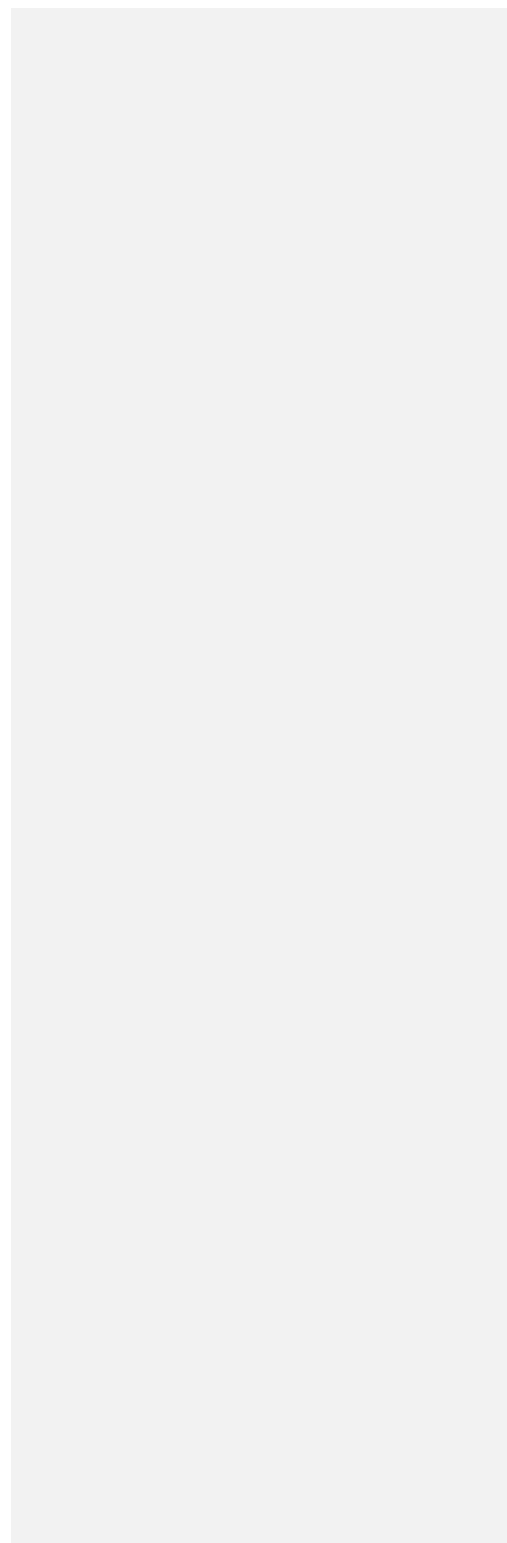
Works Cited

Barnes, C. J., & Allison, G. B. (1983). The distribution of deuterium and 18O in dry soils. 1. Theory. *Journal of Hydrology*, *60*, 141–156.

Beyer, M., Kühnhammer, K., & Dubbert, M. (2020). In situ measurements of soil and plant water isotopes : a review of approaches , practical considerations and a vision for the future. *Hydrology and Earth System Sciences*, *24*, 4413–4440. https://doi.org/https://doi.org/10.5194/hess-24-4413-2020

Bowen, G. J., Cai, Z., Fiorella, R. P., & Putman, A. L. (2019). Isotopes in the Water Cycle: Regional- to Global-Scale Patterns and Applications. *Annual Review of Earth and Planetary Sciences*, *47*(1), 453–479. https://doi.org/10.1146/annurev-earth-053018-060220

Bowen, G. J., Putman, A., Brooks, J. R., Bowling, D. R., Oerter, E. J., & Good, S. P. (2018). Inferring the source of evaporated waters using stable H and O isotopes. *Oecologia*, *187*(4), 1025–1039. https://doi.org/10.1007/s00442-018-4192-5

Brooks, J. R., Barnard, H. R., Coulombe, R., & McDonnell, J. J. (2010). Ecohydrologic separation of water between trees and streams in a Mediterranean climate. *Nature Geoscience*, *3*(2), 100–104. https://doi.org/10.1038/ngeo722

CoAgMet, Colorado Climate Center, Colorado State University, Fort Collins, CO, USA. https://coagmet.colostate.edu/

Dawson, T. E., & Ehleringer, J. R. (1991). Streamside trees that do not use stream-water: evidence from hydrogen isotopes ratios. *Nature*, *350*(March), 335–337.

Gaj, M., Beyer, M., Koeniger, P., Wanke, H., Hamutoko, J., & Himmelsbach, T. (2015). In-situ unsaturated zone stable water isotope (2H and 18O) measurements in semi-arid environments using tunable off-axis integrated cavity output spectroscopy. *Hydrology and Earth System Sciences Discussions*, *12*(6), 6115–6149. https://doi.org/10.5194/hessd-12-6115-2015

Gaj, M., Beyer, M., Koeniger, P., Wanke, H., Hamutoko, J., & Himmelsbach, T. (2016). In situ unsaturated zone water stable isotope (2H and 18O) measurements in semi-arid environments: A soil water balance. *Hydrology and Earth System Sciences*, *20*(2), 715–731. https://doi.org/10.5194/hess-20-715-2016

Gessler, A., Bächli, L., Rouholahnejad Freund, E., Treydte, K., Schaub, M., Haeni, M., Weiler, M., Seeger, S., Marshall, J., Hug, C., Zweifel, R., Hagedorn, F., Rigling, A., Saurer, M., & Meusburger, K. (2022). Drought reduces water uptake in beech from the drying topsoil, but no compensatory uptake occurs from deeper soil layers. *New Phytologist*, *233*(1), 194–206. https://doi.org/10.1111/nph.17767

Gómez-Navarro, C., Pataki, D. E., Bowen, G. J., & Oerter, E. J. (2019). Spatiotemporal variability in water sources of urban soils and trees in the semiarid, irrigated Salt Lake Valley. *Ecohydrology*, *12*(8). https://doi.org/10.1002/eco.2154

Gonfiantini, R., Wassenaar, L. I., Araguas-Araguas, L., & Aggarwal, P. K. (2018). A unified Craig-Gordon isotope model of stable hydrogen and oxygen isotope fractionation during fresh or saltwater evaporation. *Geochimica et Cosmochimica Acta*, *235*, 224–236. https://doi.org/10.1016/j.gca.2018.05.020

Good, S. P., Noone, D., & Bowen, G. J. (2015). Hydrologic connectivity constrains partitioning of global terrestrial water fluxes. *Science*, *349*(6244), 175–177. https://doi.org/10.1126/science.aaa5931

Green, M. B., Laursen, B. K., Campbell, J. L., Mcguire, K. J., & Kelsey, E. P. (2015). Stable water isotopes suggest sub-canopy water recycling in a northern forested catchment. *Hydrological Processes*, *29*(25), 5193–5202. https://doi.org/10.1002/hyp.10706

Groh, J., Stumpp, C., Lücke, A., Pütz, T., Vanderborght, J. and Vereecken, H., (2018), Inverse estimation of soil hydraulic and transport parameters of layered soils from water stable isotope and lysimeter data. *Vadose Zone Journal*, *17*(1), pp.1-19.

Gupta, P. ,Noone, D., Galewsky, J., Sweeney, C., and Vaughn, B.H. (2009). Demonstration of high-precision continuous measurements of water vapor isotopologues in laboratory and remote field deployments using wavelength-scanned cavity ring-down spectroscopy (WS-CRDS) technology. *Rapid Com. in Mass Spectrometry Volume 23, Issue 16, Date: 30 August 2009, Pages: 2534-2542*

Harms Sarah M, & Ludwig, T. K. (2016). Retention and removal of nitrogen and phosphorus in saturated soils of arctic hillslopes. *Biogeochemistry*, *127*, 291–304. https://doi.org/10.1007/s10533-016-0181-0

Havranek, R. E., Snell, K. E., Davidheiser-Kroll, B., Bowen, G. J., & Vaughn, B. (2020). The Soil Water Isotope Storage System (SWISS): An integrated soil water vapor sampling and multiport storage system for stable isotope geochemistry. *Rapid Communications in Mass Spectrometry*, *34*(12), 1–11. https://doi.org/10.1002/rcm.8783

Hinckley, E.-L. S., Barnes, R. T., Anderson, S. P., Williams, M. W., & Bernasconi, S. M. (2014). Nitrogen retention and transport differ by hillslope aspect at the rain-snow transition of the Colorado Front Range. *Journal of Geophysical Research: Biogeosciences*, *119*, 12811896. https://doi.org/10.1002/2013JG002588

Kübert, A., Paulus, S., Dahlmann, A., Werner, C., Rothfuss, Y., Orlkowski, N., & Dubbertm Maren. (2020). Water Stable Isotopes in Ecohydrological Field Research : Comparison Between In Situ and Destructive Monitoring Methods to Determine Soil Water Isotopic Signatures. *Frontiers in Plant Science*, *11*(April), 1–13. https://doi.org/10.3389/fpls.2020.00387

Kühnhammer, K., Dahlmann, A., Iraheta, A., Gerchow, M., Birkel, C., Marshall, J. D., & Beyer, M. (2022). Continuous in situ measurements of water stable isotopes in soils, tree trunk and root xylem: Field approval. *Rapid Communications in Mass Spectrometry*, *36*(5). https://doi.org/10.1002/rcm.9232

Magh, R.K., Gralher, B., Herbstritt, B., Kübert, A., Lim, H., Lundmark, T. and Marshall, J., 2022. Conservative storage of water vapour–practical in situ sampling of stable isotopes in tree stems. *Hydrology and Earth System Sciences*, *26*(13), pp.3573-3587.

Mahindawansha, A., Orlowski, N., Kraft, P., Rothfuss, Y., Racela, H., & Breuer, L. (2018). Quantification of plant water uptake by water stable isotopes in rice paddy systems. *Plant and Soil*, *429*(1–2), 281–302. https://doi.org/10.1007/s11104-018-3693-7

Oerter, E. J., Perelet, A., Pardyjak, E., & Bowen, G. J. (2016). Membrane inlet laser spectroscopy to measure H and O stable isotope compositions of soil and sediment pore

water with high sample throughput. *Rapid Communications in Mass Spectrometry*, *31*(1), 75–84. https://doi.org/10.1002/rcm.7768

Oerter, E. J., & Bowen, G. J. (2017). In situ monitoring of H and O stable isotopes in soil water reveals ecohydrologic dynamics in managed soil systems. *Ecohydrology*, *10*(4), 1–13. https://doi.org/10.1002/eco.1841

Oerter, E. J., & Bowen, G. J. (2019). Spatio-temporal heterogeneity in soil water stable isotopic composition and its ecohydrologic implications in semiarid ecosystems. *Hydrological Processes*, *March*, 1–15. https://doi.org/10.1002/hyp.13434

Peterson, B. J., & Fry, B. (1987). Stable Isotopes in Ecosystem Studies. *Annual Reviews of Ecology and Systematics*, *18*, 293–320. http://www.jstor.org/stable/2097134 ~~REFERENC~~

Quade, M., Klosterhalfen, A., Graf, A., Brüggemann, N., Hermes, N., Vereecken, H., & Rothfuss, Y. (2019). In-situ monitoring of soil water isotopic composition for partitioning of evapotranspiration during one growing season of sugar beet (Beta vulgaris). *Agricultural and Forest Meteorology*, *266–267*(December 2018), 53–64. https://doi.org/10.1016/j.agrformet.2018.12.002

Quade, M., Brüggemann, N., Graf, A., Vanderborght, J., Vereecken, H., & Rothfuss, Y. (2018). Investigation of Kinetic Isotopic Fractionation of Water during Bare Soil Evaporation. *Water Resources Research*, *54*(9), 6909–6928. https://doi.org/10.1029/2018WR023159

Rothfuss, Y., Vereecken, H., & Brüggemann, N. (2013). Monitoring water stable isotopic composition in soils using gas-permeable tubing and infrared laser absorption spectroscopy. *Water Resources Research*. https://doi.org/10.1002/wrcr.20311

Rothfuss, Y., Merz, S., Vanderborght, J., Hermes, N., Weuthen, A., Pohlmeier, A., Vereecken, H., & Brüggemann, N. (2015). Long-term and high-frequency non-destructive monitoring of water stable isotope profiles in an evaporating soil column. *Hydrology and Earth System Sciences*, *19*(10), 4067–4080. https://doi.org/10.5194/hess-19-4067-2015

Rothfuss, Y., Quade, M., Brüggemann, N., Graf, A., Vereecken, H., & Dubbert, M. (2021). Reviews and syntheses: Gaining insights into evapotranspiration partitioning with novel isotopic monitoring methods. In *Biogeosciences* (Vol. 18, Issue 12, pp. 3701–3732). Copernicus GmbH. https://doi.org/10.5194/bg-18-3701-2021

Rozmiarek, K. S., Vaughn, B. H., Jones, T. R., Morris, V., Skorski, W. B., Hughes, A. G., Elston, J., Wahl, S., Faber, A. K., & Steen-Larsen, H. C. (2021). An unmanned aerial vehicle sampling platform for atmospheric water vapor isotopes in polar environments. *Atmospheric Measurement Techniques*, *14*(11), 7045–7067. https://doi.org/10.5194/amt-14-7045-2021

Seeger, S., & Weiler, M. (2021). Temporal dynamics of tree xylem water isotopes: In situ monitoring and modeling. *Biogeosciences*, *18*(15), 4603–4627. https://doi.org/10.5194/bg-18-4603-2021

Soderberg, K., Good, S. P., Wang, L., & Caylor, K. (2012). Stable Isotopes of Water Vapor in the Vadose Zone: A Review of Measurement and Modeling Techniques. *Vadose Zone Journal*, *11*(3), 0. https://doi.org/10.2136/vzj2011.0165

Soil Survey Staff, Natural Resources Conservation Service, United States Department of
Agriculture. Soil Series Classification Database. Available online. Accessed 09/10/2022.

Sprenger, M., Leistert, H., Gimbei, G., & Weiler, M. (2016). Illuminating hydrological processes
at the soil-vegetation-atmosphere interface with water stable isotopes. *Reviews in
Geophysics*, *54*, 674–704. https://doi.org/10.1002/ 2015RG000515

Sprenger, M., & Allen, S. T. (2020). What Ecohydrologic Separation Is and Where We Can Go
With It. In *Water Resources Research* (Vol. 56, Issue 7). Blackwell Publishing Ltd.
https://doi.org/10.1029/2020WR027238

Stumpp, C., Stichler, W., Kandolf, M. and Šimůnek, J., (2012). Effects of land cover and
fertilization method on water flow and solute transport in five lysimeters: A long-term study
using stable water isotopes. *Vadose Zone Journal*, *11*(1).

Theis, D. E., Saurer, M., Blum, H., Frossard, E., & Siegwolf, R. T. W. (2004). A portable
automated system for trace gas sampling in the field and stable isotope analysis in the
laboratory. *Rapid Communications in Mass Spectrometry*, *18*(18), 2106–2112.
https://doi.org/10.1002/rcm.1596

Vereecken, H., Amelung, W., Bauke, S. L., Bogena, H., Brüggemann, N., Montzka, C.,
Vanderborght, J., Bechtold, M., Blöschl, G., Carminati, A., Javaux, M., Konings, A. G.,
Kusche, J., Neuweiler, I., Or, D., Steele-Dunne, S., Verhoef, A., Young, M., & Zhang, Y.
(2022). Soil hydrology in the Earth system. *Nature Reviews Earth & Environment*.
https://doi.org/10.1038/s43017-022-00324-6

Volkmann, T. H. M., & Weiler, M. (2014). Continual in situ monitoring of pore water stable
isotopes in the subsurface. *Hydrology and Earth System Sciences*, *18*(5), 1819–1833.
https://doi.org/10.5194/hess-18-1819-2014

Volkmann, T. H. M., Haberer, K., Gessler, A., & Weiler, M. (2016). High-resolution isotope
measurements resolve rapid ecohydrological dynamics at the soil-plant interface. *New
Phytologist*, *210*(3), 839–849. https://doi.org/10.1111/nph.13868

Wassenaar, L. I., Hendry, M. J., Chostner, V. L., & Lis, G. P. (2008). High resolution pore water
δ2H and δ18O measurements by H2O(liquid)-H2O (vapor) equilibration laser
spectroscopy. *Environmental Science and Technology*, *42*(24), 9262–9267.
https://doi.org/10.1021/es802065s

Zhao, P., Tang, X., Zhao, P., Wang, C. and Tang, J., 2013. Identifying the water source for
subsurface flow with deuterium and oxygen-18 isotopes of soil water collected from tension
lysimeters and cores. *Journal of Hydrology*, *503*, pp.1-10

Zimmermann, U., Munnich, K. O., & Roether, W. (1966). Tracers Determine Movement of Soil
Moisture and Evapotranspiration. *Science*, *152*(3720), 346–347.
https://doi.org/10.1126/science.152.3720.346

1632
1633